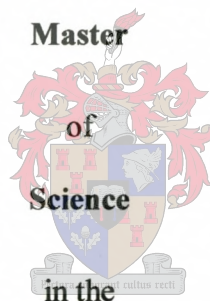


Ligand Modification of Pluronic[®] F108
for use in
Immobilized Metal Affinity Separation of Bio-Macromolecules.

By
Leon van Kralingen

Thesis

Presented in fulfilment of the requirements for the degree of



Faculty of Science
(Department of Chemistry)

at

Stellenbosch University

Promoter: Dr. H.J.A. Adendorff
Co-promoter: Dr. M.W. Bredenkamp

March 2002

Declaration

I, the undersigned, hereby declare that the work contained in this thesis is my own original work and that I have not previously in its entirety or in part submitted it at any university for a degree.

Leon van Kralingen

Abstract

In this work we aim to put into place a system to separate or immobilise bio-macromolecules by means of immobilised transition metal ions like nickel(II) or copper(II). Although the concept of immobilised metal affinity chromatography (IMAC) has been around since the early 1960's, the metal ions were always immobilised by covalent modification of the support matrix. Recently the concept of IMAC was applied to membranes, and again the metal ion was immobilised by covalent modification of the membrane surface. In this study we covalently modified the support matrix by attaching a linear, EDTA type ligand to the hydroxy end groups of a tri-block copolymer (polyethylene oxide (PEO)_{m=129} – polypropylene oxide (PPO)_{n=56} – polyethylene oxide (PEO)_{m=129}), Pluronic[®] F108. The middle block of this polymer, which is hydrophobic, will non-covalently adsorb onto the membrane surface through hydrophobic interaction. The hydrophilic outer blocks, with the ligand modified end groups, will associate with the aqueous substrate exposing the chelated metal ion for interaction with the bio-macromolecules. This affords a system which is recyclable, without replacing the membranes, simply by stripping the expired ligand modified-polymer and adsorbing fresh polymer.

A series of model ligands and their complexes were synthesised and characterised, to study the coordination of the ligand around the metal ions. The model compounds were also essential in characterising the final product – the ligand modified Pluronic.

Finally the ligand modified Pluronic was tested for its metal binding capabilities. This was done in aqueous solution by qualitatively comparing the UV-VIS spectra of the modified Pluronic with that of the model ligands and complexes. The spectra indicate that metal coordination does take place.

Uittreksel

In die studie het ons beoog om 'n sisteem daar te stel vir die skei en immobilisering van bio-makromolekules deur middel van oorgangsmetale soos nikkel(II) en koper(II). Alhoewel die beginsel van geïmmobiliseerde Metaal-ioon Affiniteits Chromatografie (IMAC) reeds sedert die vroeë 1960's bekend is, is die metaal ione geïmmobiliseer deur kovalente modifikasie van die draermaterial. Onlangs is die beginsel van IMAC uitgebrei na membrane en ook hierin is die metaalione geïmmobiliseer deur kovalente modifikasie van die membraanoppervlaktes. In die projek het ons die draermateriaal kovalent gemodifiseer deur 'n lineêre EDTA-tipe ligand te koppel aan die hidroksie eindgroepe van 'n tri-blok ko-polimeer (poli-etileen oksied (PEO)_{m=129} – poli-propileen oksied (PPO)_{n=56} - poli-etileen oksied (PEO)_{m=129}), Pluronic® F108. Die middelste blok van die polimeer, wat hidrofobies is, sal nie-kovalent aan die membraan oppervlakte adsorbeer d.m.v hidrofobiese interaksie. Die hidrofiliese buite blokke, met die ligand-gemodifiseerde eindgroepe, sal assosieer met die waterige substraat en die metal ioon blootstel vir interaksie met die bio-makromolekules. Dit stel dus 'n sisteem in plek wat herbenut kan word, sonder om die membrane te vervang, deur eenvoudig die ligand-gemodifiseerde polimeer wat verval het te stroop en te vervang met nuwe polimeer.

'n Reeks model ligande en hul komplekse was gesintetiseer en gekarakteriseer om die koördinasie van die ligande rondom die metaal ione te bestudeer. Dié model verbindings was van groot belang in die karakterisering van die finale produk – die ligand-gemodifiseerde Pluronic.

Laastens is die ligand-gemodifiseerde Pluronic getoets vir sy metaal bindings vermoë. Dit is gedoen deur die UV-VIS spectra van die gemodifiseerde Pluronic kwalitatief te vergelyk met die spectra van die model ligande en komplekse, in waterige oplossings. Die spectra dui aan dat metaalbinding wel plaasvind.

I dedicate this work to my parents to whom I am deeply indebted for their continuous support and giving me the opportunity to have come this far, I love you very much. Also to my girlfriend Marié who has been with me every step of the way, thank you for all your love and patients.

Acknowledgements

I would like to acknowledge and express my sincere gratitude to the following people and institutions.

- ❖ My promoters Dr. H.J. Adendorff and Dr. M.W. Bredenkamp for their guidance and support during this project.
- ❖ Dr. E.P. Jacobs and Prof. P. Swart for making this project possible and the rest of the AFFSEP group for their support.
- ❖ Dr. M. Rautenbach for her guidance in the peptide synthesis.
- ❖ Dr. T. van der Merwe for the ES-MS analysis.
- ❖ Dr. P. Verhoeven for the assistance in the IR and MS analysis.
- ❖ The Water Research Commition (WRC) for their financial support.
- ❖ Stellenbosch University for its financial support though various bursaries.

Table of Contents

1. Introduction	
1.1. Immobilised metal affinity chromatography – The principles	1
1.1.1. The support matrix	2
1.1.2. Activation of the support matrix	3
1.1.3. Immobilising ligands, metal ions and amino acids	5
1.1.4. Factors that influence the efficiency of IMAC	8
1.2. Immobilised metal affinity membranes (IMAM)	14
1.3. This work in context	16
1.4. Goals	18
2. Discussion	
2.1. Model ligands, reactions and ligand modification of Pluronic® F108	19
2.2. Model complexes	31
2.3. Metal binding capabilities of the ligand modified Pluronic® F108	33
3. Experimental	
3.1. Reagents	37
3.2. Solvents	37
3.3. Physical measurements	39
3.4. Tests for free amino groups and amines.	40
3.5. Synthesis of the model ligands	41
3.5.1. Diethyl <i>N,N'</i> -dicarboxymethyl-3,6-diazaoctanedioate (DEDDO)	41
3.5.2. Dimethyl <i>N,N'</i> -dicarboxymethyl-3,6-diazaoctanedioate (DMDDO)	41
3.5.3. Model reactions for determining the reaction condition and reagent addition sequence to couple the ligand to Pluronic® F108	41
3.5.4. Bis[2-(2-methoxyethoxy)ethyl <i>N,N'</i> -dicarboxymethyl-3,6-diazaoctanedioate (BMDDO)	43
3.5.5. L-Histidyl-L-histidine methyl ester (His2)	43
3.5.6. L-Histidyl- L-histidyl-L-histidine methyl ester (His3)	45

3.6. Synthesis of the model complexes	47
3.6.1. Diethyl- and dimethyl <i>N,N'</i> -dicarboxymethyl-3,6-diazaoctanedioate copper(II) complex (CuDEDDO and CuDMDDO)	47
3.6.2. Diethyl- and dimethyl <i>N,N'</i> -dicarboxymethyl-3,6-diazaoctanedioate nickel(II) complex (NiDEDDO and NiDMDDO)	47
3.6.3. Ethylenediaminediacetic <i>N,N'</i> -diacetato nickel(II) and copper (II) complexes (NiEDDA and CuEDDA)	48
3.6.4. Diethyl <i>N,N'</i> -dicarboxymethyl-3,6-diazaoctanedioate diimidazole nickel(II) complex (NiDEDDO)(Im) ₂	49
3.7. Modification of the hydroxy end groups of Pluronic [®] F108 to methyl- <i>N,N'</i> -dicarboxymethyl-3,6-diazaoctanedioate	50
3.8. UV-VIS spectroscopy	51
4. Results	
4.1. NMR results	52
4.2. X-Ray diffraction data and crystal structures	63
4.2.1. CuDMDDO	63
4.2.2. NiDMDDO(Im) ₂	66
4.3. Infra Red spectroscopy	69
4.4. Mass spectroscopy	75
4.4.1. Electron Impact Mass Spectroscopy (EI-MS)	75
4.4.2. Electrospray Mass Spectroscopy	76
4.5. UV-VIS spectroscopy	80
5. Conclusion	85
6. Future work	86
References	
Appendix	

Acronyms and abbreviations.

a	Absorptivity ($\text{cm}^{-1}\text{g}^{-1}\text{l}$)
A	Absorption
BMDDO	Bis[2-(2-methoxyethoxy)ethyl] <i>N,N'</i> -dicarboxymethyl-3,6-diazaoctanedioate
Da	Dalton
DCC	Dicyclohexanecarbodiimide
DEDDO	Diethyl <i>N,N'</i> -dicarboxymethyl-3,6-diazaoctanedioate
DEGM	Diehylene glycol monomethyl ether
DIPCDI	Diisopropylcarbodiimide
DIPEA	Diisopropylethylamine
DMDDO	Dimethyl <i>N,N'</i> -dicarboxymethyl-3,6-diazaoctanedioate
DMF	Dimethylformamide
ϵ	Molar absorptivity ($\text{cm}^{-1}\text{mol}^{-1}\text{l}$)
EDDA	Ethylenediaminediacetic acid
EDTA	Ethylenediaminetetraacetic acid
EI-MS	Electron Impact Mass Spectrometry
ES-MS	Electro Spray Mass Spectrometry
Fmoc-	Fluoronylmethyloxycarbonyl-
His2	L-Histidyl-L-histidine methyl ester
His3	L-Histidyl-L-histidyl-L-histidine methyl ester
HOBt	1-Hydroxybenzotriazole
ICP-MS	Inductive Coupled Plasma Mass Spectrometry
IDA	Iminodiacetic acid
Im	Imidazole
IMAC	Immobilised Metal Affinity Chromatography
IMAM	Immobilised Metal Affinity Membrane
IR	Infra Red spectroscopy
MMDDO	Methyl [2-(2-methoxyethoxy)ethyl] <i>N,N'</i> -dicarboxymethyl-3,6-diazaoctanedioate
μS	Micro Siemens
NMR	Nuclear Magnetic Resonance
NTA	Nitrilotriacetic acid
PEO	Polyethylene oxide
ppm	Parts per million
PPO	Polypropylene oxide
tBoc	t-Butoxycarbonyl-
TEA	Triethylamine
THF	Tetrahydrofurane
UV-VIS	Ultraviolet - Visible spectroscopy

Chapter 1: Introduction.

This chapter is divided into four sections. In the first section the principles involved in immobilised metal affinity chromatography (IMAC) are introduced. Most of these principles are valid for the system discussed in the second section, immobilised metal affinity membranes (IMAM). The third section describes the context of this research in relation to IMAC and IMAM. Section four outlines the goals set out for this project.

1.1. Immobilised metal affinity chromatography (IMAC) – The principals.

Porath and co-workers first introduced IMAC in 1975.[1] This technique rests on the principle that bio-molecules, like proteins and enzymes have an affinity towards borderline to soft transition metal ions like Co^{2+} , Ni^{2+} , Cu^{2+} and Zn^{2+} . This affinity is due to electron donating groups like the nitrogen atoms in histidine's imidazole pendant group, the indoyl group of tryptophan and the sulphur atoms in the thiol group of cysteine. Some of the most important factors that determine the relative affinity and thus retention of different bio-molecules are the amount, spacing between and topography of the electron donating amino acids.[2;3] The higher the number of accessible amino acids the greater the chance of interaction with the immobilised metal ion will be, but it is important that the electron donating groups of the amino acids are on the outside of the three dimensional structure of the protein. If two histidine residues are close enough to each other they can both co-ordinate with the metal ion leading to greater retention.[2;3] Expressing the recombinant protein with a poly-histidine affinity tag linked to its N- or C-terminus can also increase affinity due to an exposed series of neighbouring histidine residues. These factors will be discussed in greater detail in 1.1.4 (d).

Factors such as pH, ionic strength of the solution, salt type and concentration, temperature, solvent type, support matrix, linker molecules, type of ligand used and type of metal ion used may also play an important role.

Proteins are usually eluted by changing the salt concentration, decreasing the pH or increasing the gradient of a competitive agent, such as imidazole or histidine in the buffer solution.

IMAC illustrates several advantages over other methods of chromatography. Specific separation methods can be customised, by varying the type of metal ion for the type of protein to be separated. The protein typically retains its biological activity after elution from the column.

Another application of IMAC columns is the sterilisation of solutions by passing them through metal free columns to remove the metal nutrients needed for bacteria to survive.

Below is a schematic representation of an IMAC system. Each of the components of this system, as well as the factors that influence its efficiency will be discussed in the following sections.

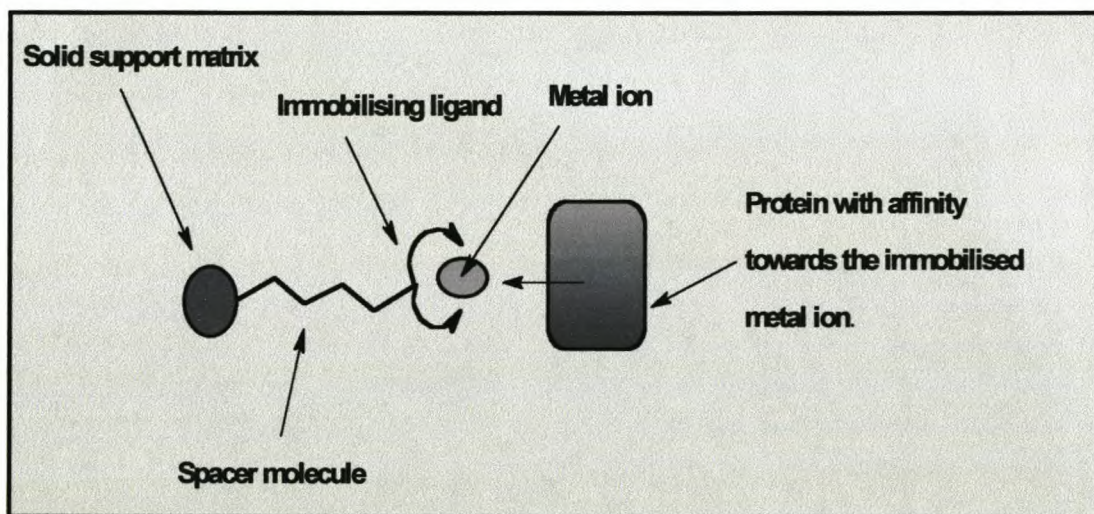


Figure 1.1.1: Schematic representation of IMAC

1.1.1. The support matrix.

Any chromatographic support must fulfil the following requirements. The particles should be of uniform size to ensure good column packing. Irregularly shaped particles may result in uneven packing and resultant band broadening. Another factor

related to particle size is flow resistance. If the particles are too small flow resistance will be high and the column may become clogged. On the other hand, if particles are too large flow resistance will be low which can lead to a loss in efficiency. Finally a large surface area is required for a high capacity as well as good mechanical stability and the support matrix should not be prone to attack by micro-organisms.[3]

One commonly used support matrix is agarose, a polysaccharide that is composed of 1,3 -linked β -D-galactose and 3,6 -anhydro- α -L -galactose units. It is water-soluble but sets at temperatures below 50°C.[3] Some of the commercial names for agarose are Sepharose[3-6] and Novarose.[7;8] Abudiab *et al.* used magnetic agarose beads, with a ferromagnetic core, to aid in post adsorption separation. This means that the peptides can be separated and washed by means of a magnet.[9]

Liesiene *et al.*[10] used a cellulose based chelating support, Chelat-Granocel. Its retention of proteins is not as strong as that of agarose based supports, which is a useful feature for large scale work, since less drastic elution conditions (change in pH) are required to remove the adsorbed proteins. With agarose based separations displacer molecules like imidazole has to be used.

Recently Zeng *et al.* used a functionalised polyacrylic acid (PAA) stationary phase to purify poly-histidine tagged recombinant proteins.[11]

A high performance, hydrophilic resin-based material with large pore size, TSK-gel chelate-5PWE is also available for use in high performance IMAC (HPIMAC).[12-14] The TSK-gel is sold with the immobilising ligand already attached to the support, but the type of ligand is not specified by the manufacturer.[14] It offers satisfactory resolution and an acceptable lifetime, but its capacity is lower than that of agarose-based supports and in terms of metal (Zn^{2+} and Ni^{2+}) leakage at neutral pH, it also seems to be inferior to agarose based supports.[12] The loss of capacity is due to its lower porosity, which has a marked influence on the accessibility of the ligand.[12;13]

Haupt and co-workers used iminodiacetic acid (IDA) linked to monomethoxy polyethylene glycol 5000 (m-PEG 5000) as the support matrix in high performance capillary electrophoresis IMAC.[15]

Micro-particulate, hydrophilically coated, wide-pore silica gels have also been used in HPIMAC.[3;16;17] El Rassi and co-workers were able to link IDA to this support for HPIMAC. These silica and synthetic polymer based supports have greater mechanical stability and a more rigid structure that leads to smaller volume changes during use. However, mixed mode interaction, like silanophilic interaction, was experienced at low ionic strengths.[17] Other side effects like silanol formation at high and low pH may also be encountered.[3]

1.1.2. Activation of the support matrix.

Activation of the solid support entails the covalent linking of one end of a spacer molecule to the support, while the other end contains a chemically active group for reaction with the ligand molecule. In this way the immobilising ligand can be attached to the support matrix.

A commonly used method for the activation of agarose and cellulose based supports is that of Porath and Olin.[18] It utilises epichlorohydrin to react with the hydroxy groups on the surface of the support. The free end of this spacer molecule has a reactive epoxy group that can react with the amines in the immobilising ligand, so tethering the ligand to the support (see Fig. 1.1.2.1).[6;10;18-22]

In a similar way a diepoxide, 1,4 -butanediol diglycidyl ether can be used as a spacer, with one epoxide group first reacting with the support and the other then reacting with the amine group in the ligand.[1;9;23]

El Rassi *et al.* used, 3-glycidoxypropyltrimethoxysilane to react with their wide-pore micro-particulate silica support after which the ligand was coupled through the free epoxy group.[16;17]

Other stationary phases like Chelating Sepharose Fast Flow (Streamline) that is used in expanded bed adsorption (EBA) and TSK-gels are supplied with a metal immobilising ligand already tethered to it.[24-27]

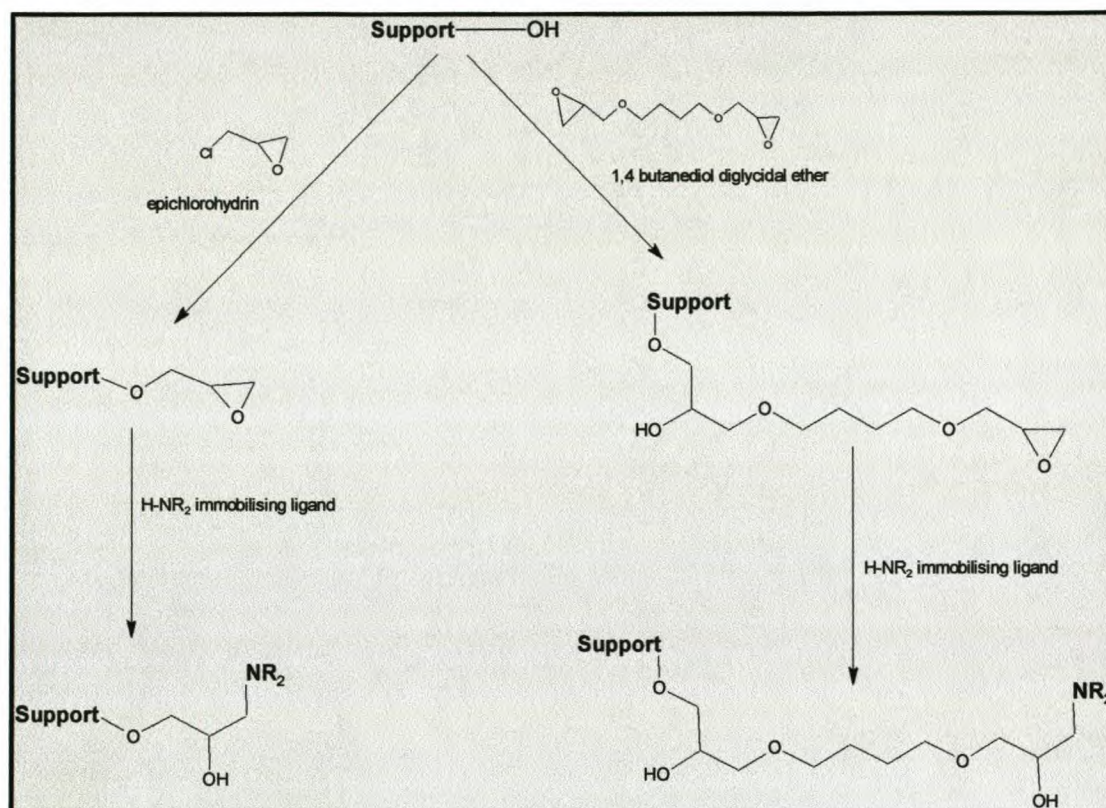


Figure 1.1.2.1: Two different ways for activating surface hydroxy groups of the support matrix.

1.1.3. Immobilising ligands, metal ions and amino acids.

The choice of ligands and metal ions for IMAC can be rationalised with the use of Pearson's hard-soft acid-base theory. In this theory the metal ion is defined as the Lewis acid, accepting electrons from the ligand, which is defined as the Lewis base. These can be further subdivided into hard and soft acids and hard and soft bases. The hardness or softness is related to the polarisability of the interacting ions. Hard acids tend to coordinate with hard bases and the same for soft acids and bases. The monovalent ions Ag^+ , Au^+ , Hg^+ , and Cu^+ are examples of soft acids, while K^+ , Na^+ , Ca^{2+} , Mg^{2+} , Fe^{3+} are classified as hard acids. Co^{2+} , Ni^{2+} , Cu^{2+} and Zn^{2+} represent the borderline acids. Hard bases include ammonia, amines, sulphates, carbonates, phosphates and perchlorates, while sulphur containing groups and the cyanide anion

are found among the soft bases. When one looks at amino acids there are three groups that can be classified as hard bases. These are the oxygen containing carboxylate amino acids (aspartic- and glutamic acid), the aliphatic nitrogen amino acids (asparagine and glutamine) and the phosphorylated amino acids, which contain phosphates. Among the borderline amino bases are the aromatic nitrogen amino acids (histidine and tryptophane), while sulphur-containing cysteine can be classified as a soft base. From this the predominant use of borderline metal ions in IMAC becomes obvious in their preferred interaction with the borderline and soft amino acids.[3;18]

It has been mentioned earlier that the immobilising ligand should coordinate the metal ion in such a way as to leave co-ordination sites vacant for interaction with the bio-macromolecule, yet the chelation must be strong enough to prevent metal ion leakage from the column or metal ion transfer (MIT)[28] from the stationary phase to the protein.

In 1975 Porath introduced iminodiacetic acid (see Fig. 1.1.3.1) as the first ligand to be used in IMAC[1]. This tridentate ligand occupies three positions of the metal's co-ordination sphere. In an octahedral co-ordination sphere there will be three unoccupied positions, while in the case of Cu^{2+} , there will only be one. Some metal leakage (Ni^{2+} , Zn^{2+}) has been experienced with the use of this ligand.[29] To circumvent this problem ligands with a higher denticity were produced.[30]

Two ligands of higher denticity that stand out are, nitrilotriacetic acid (NTA)[2] and tris(carboxymethyl)ethylenediamine (TED).[18] NTA is a tetradentate and TED a pentadentate ligand. These ligands bind the metal ion more strongly than IDA, but there is a loss in protein affinity as a result of the smaller number of co-ordination sites available for interaction. Ligands like these can be useful where high affinity, metal-scavenging proteins are considered. Porath has suggested a protein affinity series for metal chelated carboxymethylated amines which follow the order: IDA >, *N*-carboxymethylated aspartate >, TED >, *N,N',N'',N''',N''''*-carboxymethyl tetraethylenepentamine.[31]

Ligands that have been introduced more recently include tris(2-aminoethyl)amine (TREN)[7], *N*-(2-pyridylmethyl)aminoacetate,[6] hydroxamate[32] and α -aminoacyl

hydroxamate[20] ligands for Fe^{3+} , Ce^{3+} and Al^{3+} , as well as carboxymethylated aspartic acid (CM-ASP) for Ca^{2+} applications.[33]

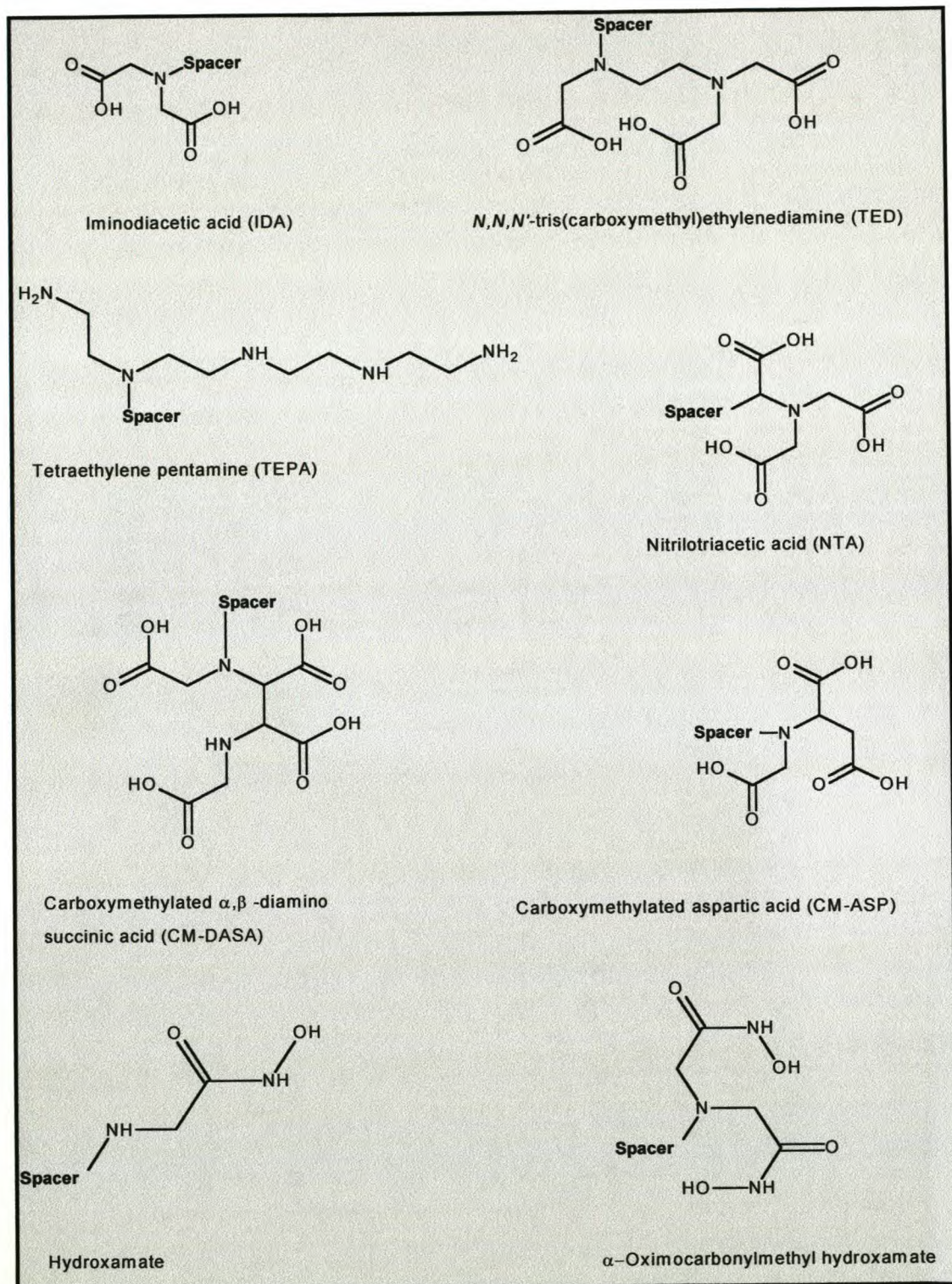


Figure 1.1.3.1: Some common immobilising ligands found in IMAC.

1.1.4. Factors that influence the efficiency of IMAC

There are a number of factors that influence the retention behavior of proteins in an IMAC column. Some of these will now be considered.

a) Metal ions. The relative affinities of the borderline metal ions for proteins can be explained qualitatively by the affinity that the metal ion has for imidazole in free solution. The stability constants follow the order: $\text{Cu}^{2+} > \text{Ni}^{2+} > \text{Zn}^{2+} \sim \text{Co}^{2+}$. The affinity of Cu^{2+} for imidazole is fifteen times that of Ni^{2+} ($\log K = 4,2$ vs. $3,0$), whose affinity in turn is more than three times that of Zn^{2+} and Co^{2+} . Higher affinities do not always translate into better separations. In the case of single-stage separation or partitioning, high binding affinities are preferred, whereas in multiple-stage chromatographic resolution weaker interaction can lead to higher selectivity.[6;30;31;34]

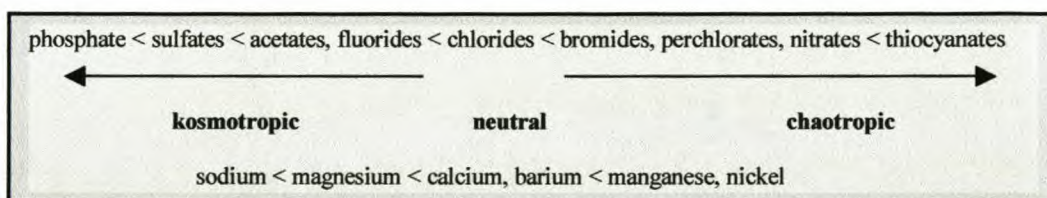
Complexes of metal ions with electrons in the e_g orbitals are normally labile. For example, Fe^{3+} with its five unshared electrons in a $(t_{2g})^3(e_g)^2$ configuration, forms labile outer sphere complexes. When this is compared with Ni^{2+} that has a d^8 $(t_{2g})^6(e_g)^2$ configuration, it is noted that Ni^{2+} forms inert complexes. This is due to the large ligand field stabilisation energy gained as a result of the splitting caused by the ligands in the protein, whereas Fe^{3+} has no ligand field stabilisation. In terms of Lewis acid-base theory Fe^{3+} is considered a hard acid and when used in IMAC its interactions will be electrovalent and charge controlled whereas the borderline Ni^{2+} prefers covalent interactions.[18]

When Fe^{3+} and other hard acids like Al^{3+} , Ca^{2+} , Yb^{3+} are used in IMAC they act more like ion exchangers. Low ionic strength buffers are usually used with these types of metals and the type of ion exchange can be modulated by changing the pH. These metals are very oxophilic and readily form hydroxide complexes. By varying the hydroxide concentration the charge on the metal complex can be controlled to be either positive (anion exchanger) or negative (cation exchanger). The pH thus determines the net charge on the protein. Separation is achieved by coulombic interaction between the protein and the immobilised complex. This adds an extra dimension to IMAC.[18;20;32;33;35-38]

b) pH: Metal co-ordination and adsorption/desorption of the protein can be controlled by varying the pH.[39] Most of the IMAC ligands have carboxymethyl groups that need to be deprotonated in order to chelate with the metal ion. This is usually achieved at pH of 4 or higher. The pendant groups of the coordinating amino acids (His and Cys) also need to be deprotonated in order to interact with the metal ion. The pK_a of these residues will differ from protein to protein, but it usually lies between 6 and 8. The adsorption of proteins is achieved under more basic conditions and elution/desorption under more acidic conditions. The influence of pH, with the use of hard metal ions, has been discussed in the previous section.

c) Salt effects: The role of the salt concentration is twofold. The first of these is to cancel electrostatic interaction by providing an ample supply of counter ions. Without a high salt concentration, the immobilised metal moiety would basically act as an ion exchange resin. Salt concentrations are usually in the range of 0,1 – 4M.

The other function of the salt is to structure the water molecules. This is achieved by the use of kosmotropic salts, which can be arranged in a lyotropic or Hofmeister series according to their abilities to precipitate proteins from an aqueous solution.



Changing the structure of the water molecules enhances the hydrophobic interactions of the protein. Due to this effect the protein is forced out of the solvent onto the support matrix. This brings the protein in close proximity with the metal ion where short-range forces can come into play. Coordination can take place when the electron donating groups penetrate the outer coordination sphere of the metal ion, enabling charge transfer. Kosmotropic salts also protect the protein against denaturation and promote refolding of denatured proteins. Salts that are usually used are NaCl, NH₄Cl, and Na₂SO₄. [3;17;18;30;40-43]

d) Amino acids: Histidine plays the prominent role in the retention of proteins in an IMAC column. The other amino acids can play a secondary or indirect role in the affinity retention of a protein. The pK_a values of histidine residues can be influenced by vicinal, charged amino acids, steric hindrance by bulky pendant groups and the hydrophobicity of the protein.[28;30]

The importance of the number, spacing and topography of histidine residues in the retention behaviour of proteins was summarised by Sulkowski[28] in terms of an IDA-M(II) stationary phase (see Table 1.1.4.1).

1. An absence of surface histidine residues correlates to a lack of retention in an IDA-M(II) column.
2. When there is one surface histidine available for coordination it results in retention on an IDA-Cu(II) column.
3. The presence of two surface residues results in stronger retention on an IDA-Cu(II) column.
4. A protein must have at least two surface histidines to be retained on an IDA-Ni(II) column.
5. Multiple histidine residues should result in stronger retention on all IDA-M(II) columns.
6. For strong retention on IDA-Co(II) or IDA-Zn(II) columns, vicinal histidine residues are required. This condition is met when two histidine residues are separated by two to three units in an α -helix. Two histidine residues can also be adjacent due to appropriate folding of the protein.
7. Two vicinal histidine residues on the surface of a protein should result in stronger binding, than when the two residues are separated far from each other, on all IDA-M(II) columns.

Table 1.1.4.1: Surface histidine requirements for the different borderline, transition metal ions commonly used in IMAC.

	Cu	Ni	Zn	Co
-His-	+	-	-	-
-His-(X)n-His-	+	+	-	-
-His-(X)n-His- n = 2,3; α -helix	+	+	+	+
(-His-His-)	+	+	+	+

The selectivity for a certain protein can be enhanced by expressing the protein with an affinity handle such as (His₆₋₈)[2;22;24;44-46], a poly-histidine peptide which can either be expressed on the N- or C-terminus of the desired protein. It has already been noted that metal ions in IMAC, especially those with two vacant coordination sites, have a higher affinity towards histidine residues that are next to each other. This poly-histidine tag does not always give the desired effect because it can get tangled up in the three dimensional structure of the protein during folding. To overcome this problem new affinity tags are being developed. Kronina and co-workers synthesised synthetic peptides that should have a high affinity towards copper. These peptides form α -helices with the histidine residues all on one side.[22] Enzelberger and co-workers have done similar work by using, a mutated version of the metal binding site of *Helicobacter pylori* ATPase (heli_{M14}-tag) as affinity handle.[24]

e) Ligand density: In general a higher ligand density relates to longer retention and better resolution.[28;43] Liesiene *et al.*[10] concluded from their study of the influence of ligand density in the IMAC of human growth hormone that a high ligand density is preferred in the initial protein purification step. A lower ligand density is more suitable for deep purification of the protein. Ligand density can be modulated by (i) altering the ligand concentration in the reaction mixture when coupling the ligand to the support or (ii) changing the number of the epoxy groups (variation of the epichlorohydrin concentration during matrix activation) in the activated matrix.

f) Displacer/competing agents: A common way to desorb bound proteins is with the use of a competing agent that has a higher affinity for the metal ion than the

protein. The protein is displaced by the competing agent and eluted. The use of a selective gradient containing imidazole or histidine at low concentration (50mM) and neutral pH is an effective way of displacing bound proteins.[3] The elution order of proteins can be affected by using competing agents especially when a gradient is employed. Even strongly bound proteins, especially those coordinated to IDA-Cu(II) gels, can be displaced by employing imidazole or histidine.[17]

Johnson *et al.* used an imidazole gradient for the separation of four variants of *Saccharomyces cerevisiae* iso-1-cytochrome c.[27;39] These variants differ only in their histidine multiplicity, varying from one to four.

Fitton *et al.*[5] introduced the use of NH₄Cl, in a three-step elution purification of penicillin acylase, to obtain higher selectivity and purification. NH₄Cl is easy-to-use, very efficient for the purification of penicillin acylase and it can be employed on industrial scale.

The effectiveness of a polymeric imidazole displacer has been compared to that of the monomeric imidazole.[23;47;48] The synthetic vinyl imidazole and vinyl caprolactam copolymer [poly(VI-VCL)] were considered. These polymers are thermosensitive and precipitate quantitatively from aqueous solutions at a temperature of 48°C. This was used to elute the thermostable, (His)₆-tagged lactate dehydrogenase [(His)₆-LDH] of *Bacillus stearothermophilus* from an IDA-Cu(II) column. It was found that the polymer displaced all of the tagged protein at a concentration of 3,7mM of imidazole units. At this concentration only weakly bound proteins were eluted by monomeric imidazole. Complete elution with imidazole occurred only at a concentration of 160mM. This is probably due to the multipoint interaction of the imidazoles in the same macromolecule with one Cu²⁺ ion.

In conclusion: Immobilised metal affinity chromatography offers a very effective mechanism for separating proteins. It is a safe technique to use in the sense that the risk of denaturation and the subsequent loss of biological activity of the proteins are very low. The technique can also be customised, to obtain high selectivity and purity under any specific set of conditions, by changing a variety of factors that influence the separation.

IMAC principles can also be extrapolated to related techniques like slurry bioreactors[30], two phase aqueous affinity partitioning[30;49;50], metal affinity precipitation[30] and bio-sensors.[51]

1.2. Immobilised metal affinity membranes (IMAM).

Immobilised metal affinity membranes are essentially the same as IMAC. The difference being that the stationary phase is a flat sheet or hollow fibre membrane.[52]

In order to gain higher capacity and resolution in IMAC it is necessary to use smaller beads with an increased packing density which often results in considerable loss of pressure.[52;53]

In 1988 Brandt *et al.* proposed the use of micro-porous membranes for affinity separation. This method approaches a column having the lowest height and the widest bed cross-section, resulting in a smaller loss of pressure under high-pressure conditions. They also suggested that affinity membranes would be of greater advantage than IMAC columns due to a shorter distance of mass transfer in the micro-pores of affinity membranes.[52;53] This leads to higher throughput and faster processing. Membrane systems are also capable of handling unclarified feedstock and can so be implemented earlier in downstream processing.[54]

Kubota *et al.* showed the effective use of a cellulose acetate, micro-filtration membrane for the recovery of serum proteins. This membrane was 0,125 mm thick with a 90 mm diameter and average pore size of 0,2 μm . Base hydrolysis of cellulose acetate yielded cellulose. The hydroxy group on position six reacted with epichlorohydrin to yield the epoxy-activated membrane, which was reacted with IDA. This membrane was loaded with Cu^{2+} ions.[53]

Hari *et al.* used epichlorohydrin modified cellulose membranes to immobilise Cu^{2+} ions for the separation of human IgG.[55]

The method used by Gonzalo *et al.* [54] to activate glass, hollow fiber, micro-filtration membranes was similar to this. It involved silanisation with 3-glycidoxypropyltrimethoxysilane and subsequent reaction of the epoxy group with IDA.

Reactive surface hydroxy groups can also be obtained by using hydroxy containing monomers in the synthesis of the polymer, as is the case with polyvinylbutyral[56] and poly(2-hydroxyethyl methacrylate).[57;58]

Grasselli *et al.* [59] grafted hydrophilised polyethylene hollow fiber membranes with glycidylmethacrylate (GMA) to obtain a reactive epoxy group on these types of membranes. The epoxy group was then in turn reacted again with IDA to afford a metal chelating membrane.

In 1994, Reif *et al.* [60] compared two commercially available immobilised metal affinity membrane adsorbers (IMA-MA) available from Sartorius. The membrane itself consists of a hydrophilic copolymer carrying IDA chelating groups. They are between 170 and 190 μm thick with an average pore size of 0,45 μm and are stable in the pH range of 2 – 13. These systems offer a cheap and easy-to-handle alternative to conventional LC-IMAC columns. Up-scaling is also simple seeing that up to ten units can be stacked with a linear increase in overall capacity. The resolution obtained is comparable to that of standard IMAC columns.

Epoxy modified polysulfone hollow-fibre membranes, with IDA as chelator for Cu^{2+} , was successfully used to separate pectic enzymes in fruit juice clarification.[61] It was indicated by the authors that this system is very easy to scale up, simply by bundling the fibres. Micro-filtration hollow fibres have the added advantage of high surface area/volume ratio, reduced diffusion distance and low operating pressure over flat sheet membranes and conventional IMAC techniques. This results in high volume throughput, high ligand utilisation and low cost. It is also possible to process particle-containing solutions by means of this system.[61]

IMAM adds an extra dimension to IMAC, especially when larger volumes need to be separated. A variety of supports are available and can be cast in different forms, be it flat sheet or hollow fiber. This technique can also be applied under higher pressures and flow rates without a loss in pressure while maintaining good separation and resolution.

1.3. This work in context.

In this study we aim to take immobilised metal affinity membranes (IMAM) one step further, by tethering the metal ion non-covalently to the membrane surface and not modifying the membrane covalently. We intend to do this by modifying the hydroxy end-groups of a tri-block co-polymer that will non-covalently adsorb onto the membrane surface.

The polymer is Pluronic[®] F108 (see Fig. 1.3.1) which consists out of two hydrophilic polyethylene oxide (PEO), hydroxy terminated, outer blocks and a hydrophobic polypropylene oxide (PPO) middle block. It is through this PPO block that the polymer adsorbs onto the hydrophobic polysulfone (hollow fibre) membrane while the PEO blocks (tethers) associate with the aqueous substrate. The metal ion would be immobilised by ligands coupled to the PEO tethers, thus allowing interaction between the metal ions and the substrate. Pluronic can also act a shield to protect against non-specific adsorption of hydrophobic proteins onto the membrane surface.

This principle has already been proven by Ho and co-workers[62] by modifying Pluronic[®] F108's hydroxy end-groups with NTA and adsorbing this to polystyrene beads. The system was loaded with Ni²⁺ and histidine tagged firefly luciferase was immobilised.

This concept has not yet been extended to membranes. In order for it to be used on a large scale on membranes the modification of the polymer must be a simple and cost effective process. In this work we introduce a new type of ligand that can be coupled to Pluronic in a simple two-step, one pot reaction using inexpensive chemicals.

Figure 1.3.1. shows the envisaged final product.

Because the polymer is non-covalently adsorbed onto the membrane, it can readily be stripped from the membrane, when it has expired. The membrane can then be coated with fresh ligand-modified polymer and reloaded with metal ions, thus avoiding complete membrane replacement.

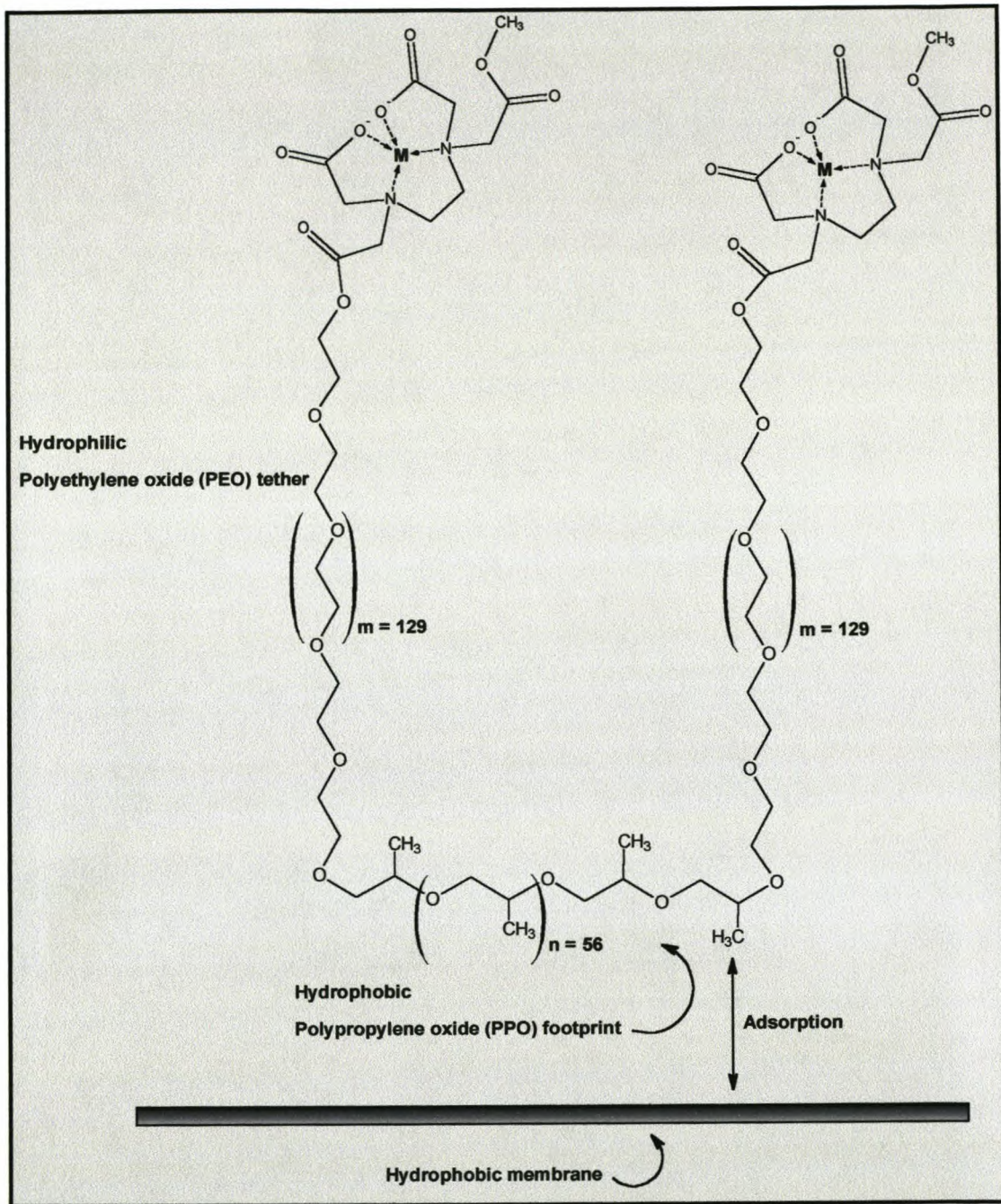


Figure 1.3.1: Schematic representation of the envisaged final product.

1.4. Goals.

The goals set out for this project were as follows:

- ◆ The synthesis and characterisation of model ligands (see 2.1 and 3.4).
- ◆ The synthesis and characterisation of model complexes and determining whether the complex complies with the requirements for IMAC (see 2.2 and 3.5).
- ◆ Coupling of the ligand to Pluronic[®] F108 (see 2.1, The support matrix, and 3.6).
- ◆ Testing whether the ligand modified Pluronic chelates metal ions (see 2.3 and 3.7, UV-VIS spectroscopy).

Chapter 2: Discussion.

This chapter will outline the choice, synthesis and characterisation of (1) the model ligands and how this led to establishing a methodology for coupling the ligand to Pluronic, (2) the model complexes and (3) the testing of the metal binding ability of the assembled system.

2.1. Model ligands, reactions and ligand modification of Pluronic[®] F108.

The choice of a suitable ligand has to take into account that the ligand must be simple, easy to prepare and relatively inexpensive since one of the projected applications involves water purification that will necessitate need for future scale up of the preparation procedure.

The most commonly used ligands in IMAC are the tripodal, tetradentate nitrilotriacetic acid (NTA) and the tridentate iminodiacetic acid (IDA). These ligands are used with Ni^{2+} (octahedral) and Cu^{2+} (square planar) ions respectively.[3]

In this work it was envisaged to investigate the linear, tetradentate, EDTA-type ligands; *diethyl and dimethyl N,N'-dicarboxymethyl-3,6-diazaoctanedioate* (DEDDO and DMDDO) as model ligands, where two of the acid groups have been converted to either ethyl or methyl esters (see Fig. 2.1.1). This was achieved by reacting the appropriate alcohol, under reflux conditions with ethylenediaminetetraacetic dianhydride (referred to as dianhydride). Ethanol was initially used, as the ethyl group would simulate the first node of Pluronic. However, in order to make the ligand simpler and lessen steric hindrance, methanol was substituted for ethanol. It was assumed that this would give better X-ray crystal structures due to the decrease in disorder of the methyl group compared to the ethyl group. This was indeed observed later with the copper complex. The reaction with methanol also had a higher yield.

The only precedents in the literature of alcoholysis of the dianhydride is the work of Takeshita *et al.*[63;64] who reacted long chain aliphatic alcohols with one side of the

dianhydride and hydrolyse the other side with water to form asymmetrical compounds. The reaction was carried out in DMF at high temperature to dissolve the dianhydride. Yields of the sought after products were very low. The dianhydride is very inert compared to other anhydrides like acetic anhydride, and needs long reaction times at high temperatures to be susceptible to nucleophilic attack. This may account for low yields and selectivity.

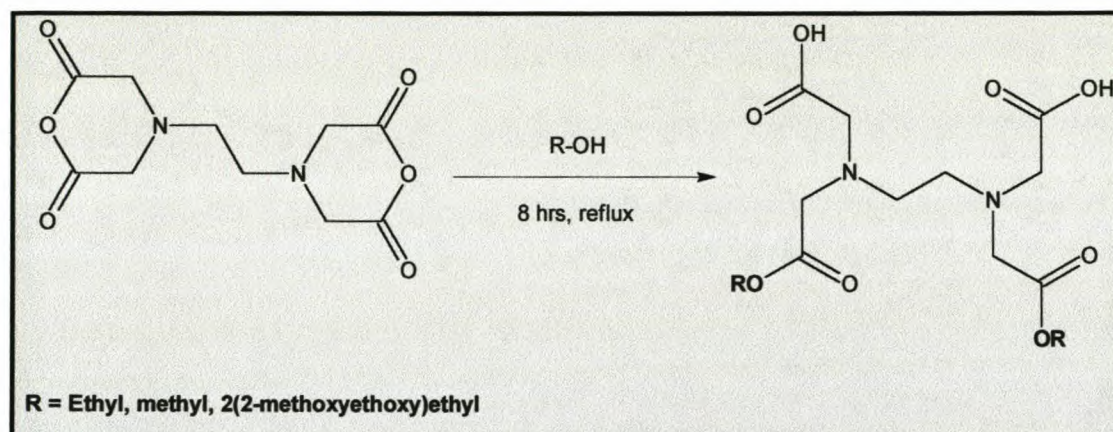


Figure 2.1.1: Synthesis of the model ligands.

An asymmetrical model ligand *methyl [2-(2-methoxyethoxy)ethyl] N,N'-dicarboxymethyl-3,6-diazaoctanedioate* (MMDDO) (see Fig 2.1.2) (diethyleneglycol monomethyl ether (DEGM) forming the ester on one side and a methyl ester on the other side of the molecule) was also synthesised in order to determine the reaction conditions and addition sequence of the reagents needed to couple the ligand to Pluronic. DEGM was chosen as it simulates the first two nodes of the PEO tether of Pluronic and because it would be easier to handle and characterise than the bulky Pluronic. The chemical reactivity of the hydroxy group in DEGM should be similar to the terminal hydroxy groups of Pluronic.

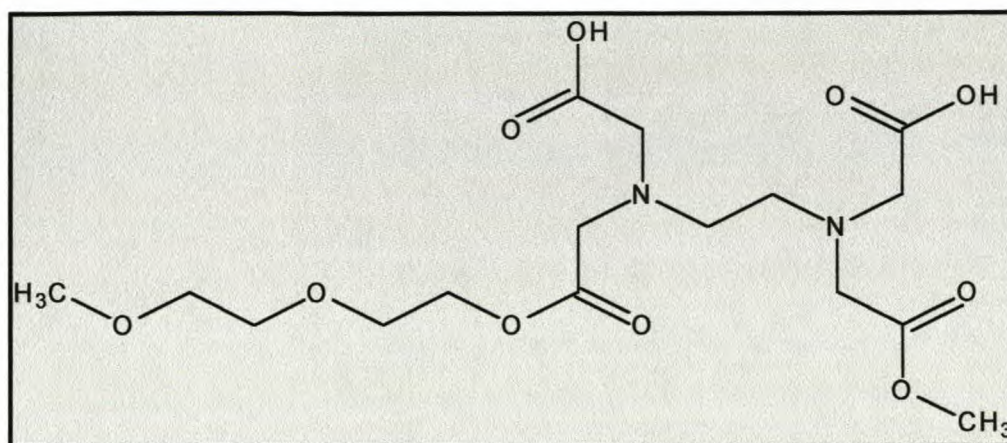


Figure 2.1.2: The asymmetrical model ligand *methyl [2(2-methoxyethoxy)ethyl] N,N'-dicarboxymethyl-3,6-diazaoctanedioate (MMDDO)*

Four reaction procedures that have led to the development of a successful reaction protocol for coupling the ligand to Pluronic are discussed next in each of the four procedures, the most successful reaction for that specific step in the developing process is described.

The choice of solvent is very important. The solvent should not be able to react with the anhydride groups and it must be completely free of moisture as water will hydrolyse the anhydride groups. The only solvent available that would dissolve the dianhydride without reacting with the anhydride groups was DMF.[63] The DMF had to be distilled (see Chapter 3.2) to ensure that it was completely dry. DMF was only able to dissolve the dianhydride at fairly high temperatures ($> 80^{\circ}\text{C}$). This posed a problem because methanol had to be added in one of the steps during the coupling reaction of the ligand to Pluronic. At this temperature methanol would evaporate from the reaction mixture, but on the other hand methanol needs high temperatures (reflux) to react with anhydride groups as can be seen in the synthesis of the model ligands DEDDO and DMDDO.

In the first two procedures DEGM was reacted with the dianhydride in DMF to form the one half of the asymmetrical ligand, MMDDO, after which the DMF was removed and the residue reacted with methanol, by using methanol as the solvent, to form the second half.

In the third and fourth procedure DEGM was still added first but the DMF was only removed after the reaction with methanol. Here imidazole was used to activate the anhydride groups (forming the bisimidazolide intermediate) towards nucleophilic attack from the hydroxy groups (see Fig. 2.1.3).[64] This also resulted in the dianhydride being dissolved at a much lower temperature (30 – 40°C). Methanol could now be added to the DMF mixture in the second step of the coupling process without it evaporating and still be able to react with the anhydride group.

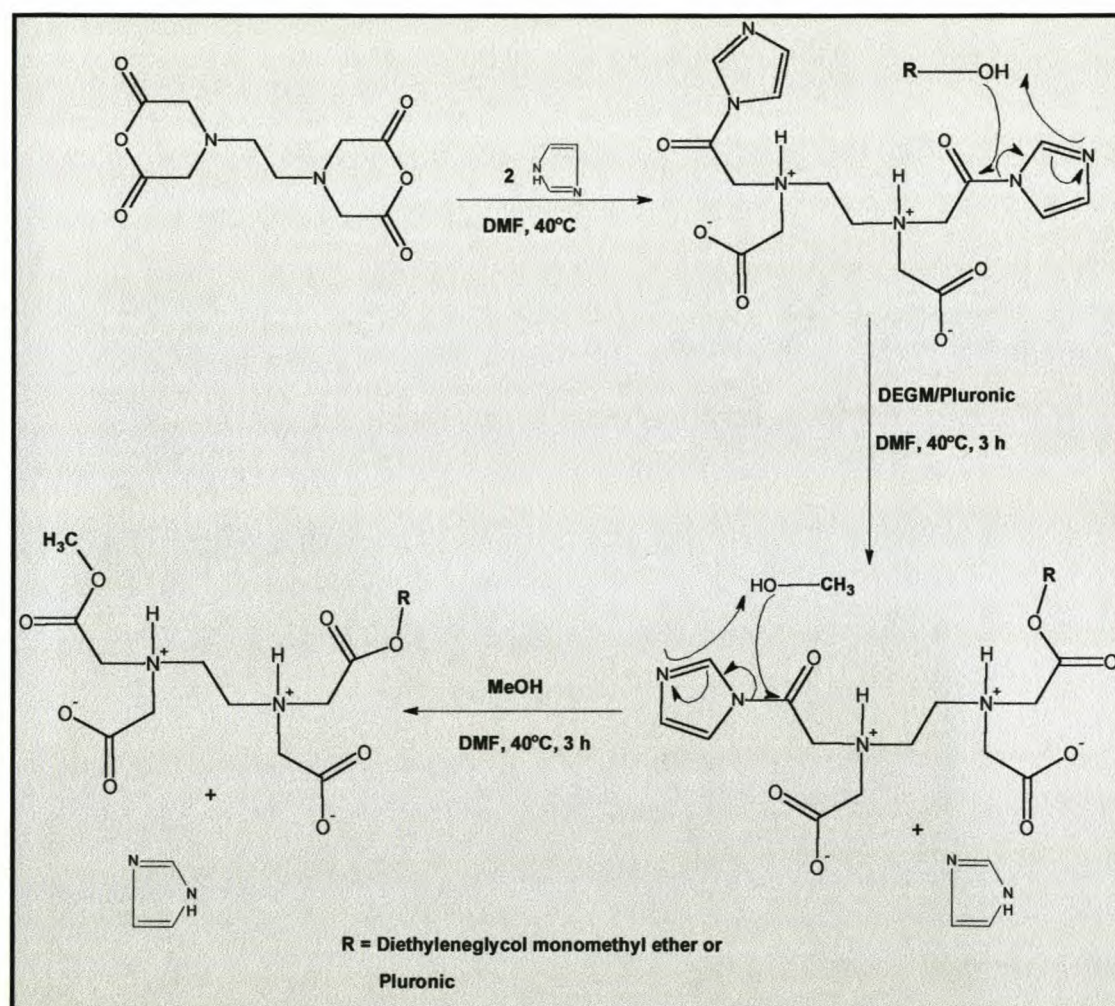


Figure 2.1.3: The activation of the anhydride groups by imidazole.

First procedure: This was the first attempt to synthesise the asymmetric model ligand MMDDO. DEGM was made a stronger nucleophile by deprotonating the hydroxy group with NaH, forming the sodium salt of DEGM, before it was added in stoichiometric amounts to the dianhydride solution. The dianhydride was dissolved in dry DMF by heating the mixture to 80°C. This mixture was reacted for 3 h at 40°C

after which the DMF was evaporated and methanol added and heated under reflux conditions to react with the remaining anhydride groups. From Electro Spray Mass Spectrometry (ES-MS) spectra it was clear that the desired product did form but that by-products like DMDDO, bis[2-(2-methoxyethoxy)ethyl] *N,N'*-dicarboxymethyl-3,6-diazaoctanedioate (BMDDO) and EDTA were also obtained. Due to the similarities in structure of these compounds it was not possible to separate them from each other.

Second procedure: In a next attempt, to obtain a simpler product mixture and to ascertain whether it was necessary to deprotonate DEGM, a two-fold excess of the dianhydride, with respect to DEGM, was reacted in DMF at 80°C after which the DMF was removed and the residue was refluxed in methanol. The ES-MS spectra of the final product mixture indicated the presence of mainly DMDDO and to a lesser extent the desired MMDDO and unreacted DEGM and not the expected 1:1 ratio of MMDDO to DMDDO. This could be because the DEGM is not as reactive towards the dianhydride as methanol. DEGM is also present in much lower concentrations, in the reaction mixture, than methanol (as a solvent in the second step). Furthermore, transesterification can also take place during the last step in the synthesis where DEGM ester is replaced by methanol.

Third procedure: In order to overcome the problems of the previous attempt it was decided to use imidazole to activate the dianhydride toward nucleophilic attack. In this way the dianhydride could be dissolved at a much lower temperature (30 - 40°C). The sodium salt of DEGM was used to react with the dissolved activated dianhydride after which methanol was added. The ES-MS spectra indicated that MMDDO formed in greater quantities than in the previous attempts but there was still a significant amount of by-products (BMDDO and DMDDO) present in the final product mixture.

Fourth procedure: From the previous reaction it seemed unnecessary to use the combination of imidazole and the sodium salt of DEGM. The alkoxy salt seems to be too reactive in combination with the bisimidazolide resulting in a loss of control and the by product, BMDDO, forming.

It was decided to use DEGM, and not the sodium salt of DEGM, to react with the bisimidazolide under similar conditions as in the previous reaction. ES-MS spectra

indicated the formation of mainly the desired product and to a lesser extent the by-products DMDDO and BMDDO.

These model experiments supplied the necessary information about the reaction conditions for the coupling of the ligand to Pluronic. Working with Pluronic also has the added advantage of working with a great excess of the dianhydride. Using an excess dianhydride ensures that only one hydroxy group reacts with one dianhydride molecule. It is also relatively easy to separate the modified Pluronic from the by-product DMDDO. This was not the case with the model reactions where the desired product and the by-products are very similar in structure, which makes it very difficult to separate them, even by column chromatography. In thin layer chromatography all the components had more or less the same R_f-value for a given solvent mixture. Pluronic on the other hand is soluble in organic solvents like toluene and benzene, whereas DMDDO is only soluble in very polar solvents like water.

Coupling of the ligand to Pluronic[®] F108: The two hydroxy end groups of Pluronic were modified in a two-step reaction to yield the tetradentate DMDDO type ligand at the end of Pluronic. This reaction was carried out by dissolving a ten-fold excess of the dianhydride and imidazole in distilled DMF after which the Pluronic was added and reacted for 8 h at 40°C. Methanol was then added and reacted for another 8 h after which the DMF was removed *in vacuo*. It was decided to use longer reaction times due to the size of Pluronic. The residue was treated with toluene to selectively dissolve ligand-modified-Pluronic from the DMDDO by-product. The final product was characterised mainly by NMR (see Chapter 4.1) with the aid of the model ligands.

A by-product, *bis[2-(2-methoxyethoxy)ethyl] N,N'-dicarboxymethyl-3,6-diazaoctanedioate* (BMDDO) (see Fig. 2.1.4.), in the preceding model reactions was synthesised as a model ligand to aid with the NMR characterisation of the ligand-modified-Pluronic. DEGM simulates the first two nodes of Pluronic and the NMR spectrum of this ligand was instrumental in characterising the ligand-modified-Pluronic (see Chapter 4.1.). In this case DEGM was used instead of ethanol or methanol. This reaction was carried out in DMF.[65]

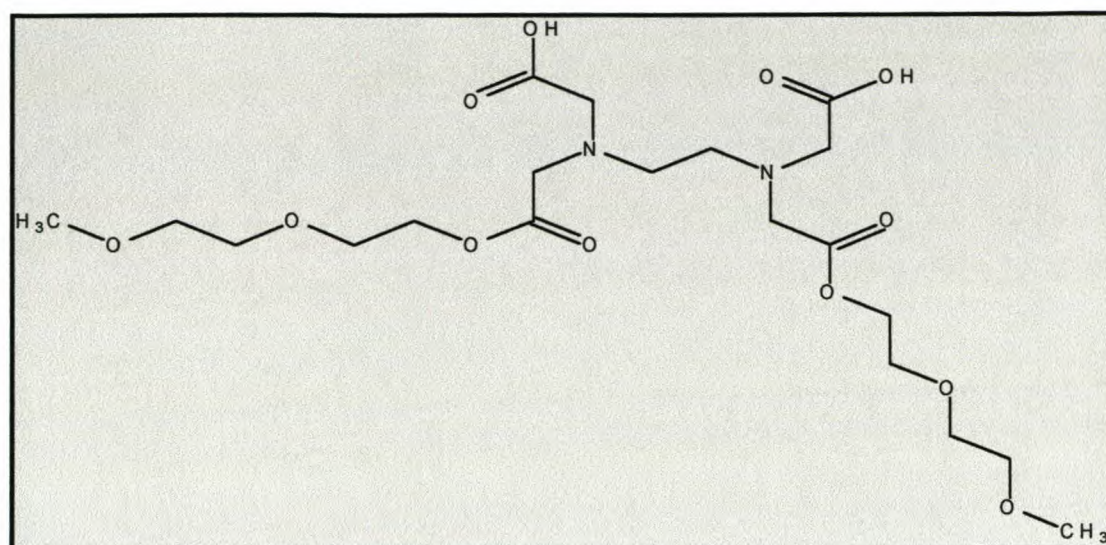


Figure 2.1.4: Bis[2-(2-methoxyethoxy)ethyl] *N,N'*-dicarboxymethyl-3,6-diazaoctanedioate (BMDDO)

EDTA was also used to compare the relevant chemical shifts with that of the model ligands and the final product.

L-Histidyl-L-histidine methyl ester (His2) and L-histidyl-L-histidyl-L-histidine methyl ester (His3) were synthesised to simulate the poly-histidine tag, which is expressed with recombinant proteins to act as an affinity handle for the separation of the protein. These di- and tri-peptides will eventually be used as a first test to determine the retention capabilities of the modified Pluronic. These peptides will also be studied in model complexes that would simulate a poly-histidine affinity tag's interaction with the metal ion.

In all of the following reactions specially prepared DMF was used. (see Chapter 3.2 for DMF preparation).

In initial attempts to synthesise His2, *N*^α-*t*-butoxycarbonylhistidine (tBOC-His) and L-histidine methyl ester dihydrochloride (His-OCH₃·2HCl) (see Fig. 2.1.7) were used as starting compounds. tBOC-Histidine's protecting tBOC group can easily be cleaved off, at the end of the reaction, by trifluoroacetic acid yielding isobutene and CO₂.^[66] It was decided to use histidine methyl ester as the other amino acid derivative in the model di-peptide, since its carboxylic acid group is protected from interaction with

metal ions. In IMAC it is usually the nitrogen atoms in the imidazole side chain of histidine that interact with the metal ion.

tBOC-His and dicyclohexylcarbodiimide (DCC)[67], which acts as a dehydration agent and aids in the peptide bond formation (see Fig. 2.1.5), were suspended in a 1:1 mixture of dichloromethane and DMF. To this was added 1-hydroxybenzotriazole (HOBt) dissolved in a small amount of DMF. HOBt acts as a 'trapping agent' preventing racemisation of amino acids during peptide formation.[68] His-OCH₃.2HCl and diisopropylethylamine (DIPEA), which acts as a base to neutralise the dihydrochloride, were dissolved in DMF and was slowly added to the tBOC-His/DCC/HOBt mixture. After 3 h not all of the reagents had dissolved, more dichloromethane was added, and the mixture was left to react overnight at room temperature. An amorphous, sticky precipitate resulted. A small sample of this was subjected to a Kaiser test for primary amines (see chapter 3.4).[68] The sample tested positive which indicated that there was unreacted His-OCH₃ present in the mixture. Thin layer chromatography (TLC) with ninhydrin (0,1% m/v ethanol solution sprayed onto the TLC plate and developed in a oven until a colour change appeared) as indicator for primary amines revealed that very little product has formed. Ninhydrin changes colour to purple in the presence of primary amines. This reaction was discontinued. The starting compounds were not completely dissolved in the suggested solvent mixture, which probably caused the ineffective coupling of the amino acids.

In a next attempt *N*^α,*N*^γ-bis(fluoronylmethoxycarbonyl)-L-histidine ((Fmoc)₂-His) (see Fig. 2.1.7) and L-His-OCH₃.2HCl were used as starting compounds. The Fmoc groups also protects against unwanted side reactions taking place on the amino groups of the histidine. The Fmoc group is base-labile and the histidine can be rapidly deprotected, under mild conditions, using piperidine, which scavenges the dibenzofulvene intermediate and thereby prevents back-addition to the peptide.[68] The peptide bond formation between the carboxylic acid group of (Fmoc)₂-His and the amino group of His-OCH₃ was assisted by the dehydrating agent diisopropylcarbodiimide (DIPCDI) (similar to DCC) and again HOBt was employed to prevent racemisation. A by product, diisopropyl urea is formed during the reaction

(see Fig.2.1.5.). The dihydrochloride was again neutralised by the proton scavenger DIPEA, which acts as a base and a very poor nucleophile due to the steric effect of the isopropyl groups. The use of DIPEA was necessary because similar bases such as triethylamine might prematurely deprotect the (Fmoc)₂-His during synthesis.

(Fmoc)₂-His and DIPCDI was dissolved in a minimum amount of DMF and to this was added HOBt, dissolved in a minimum amount of DMF. His-OCH₃.2HCl together with DIPEA was dissolved separately in DMF and added to the preceding mixture. The mixture was stirred overnight and again an amorphous, sticky residue formed. A small sample tested positive for primary amines to the Kaiser test. TLC revealed that there was still unreacted His-OCH₃ left. The reaction was left for another 3 h, after which the DMF was removed by a nitrogen stream. The residue was treated overnight with ethyl acetate resulting in a murky suspension. The undissolved residue was filtered off. The filtrate was extracted with 0,1% aqueous acetic acid solution to remove unreacted amines solution leaving only the desired product in the ethyl acetate layer. The ethyl acetate was removed under reduced pressure and the residue washed with *n*-hexane yielding a yellow, amorphous product. This was freeze-dried overnight. A small sample was treated with piperidine liberating the Fmoc protecting groups and exposing the α amino group of the coupled (Fmoc)₂-His. TLC revealed the presence of the final product. The rest of the yellow product was treated for 1 h with piperidine, during which time a white precipitate formed which was separated from the piperidine by means of a centrifuge. The white precipitate (His₂) was washed three times with ether and freeze-dried.

This procedure has limitations due to the formation of the amorphous, sticky intermediates and the subsequent loss in yield. Yields for this procedure were less than 30%. Higher yields are needed if the product (His₂) is to be used in studying the model complexes and testing the performance of the affinity system.

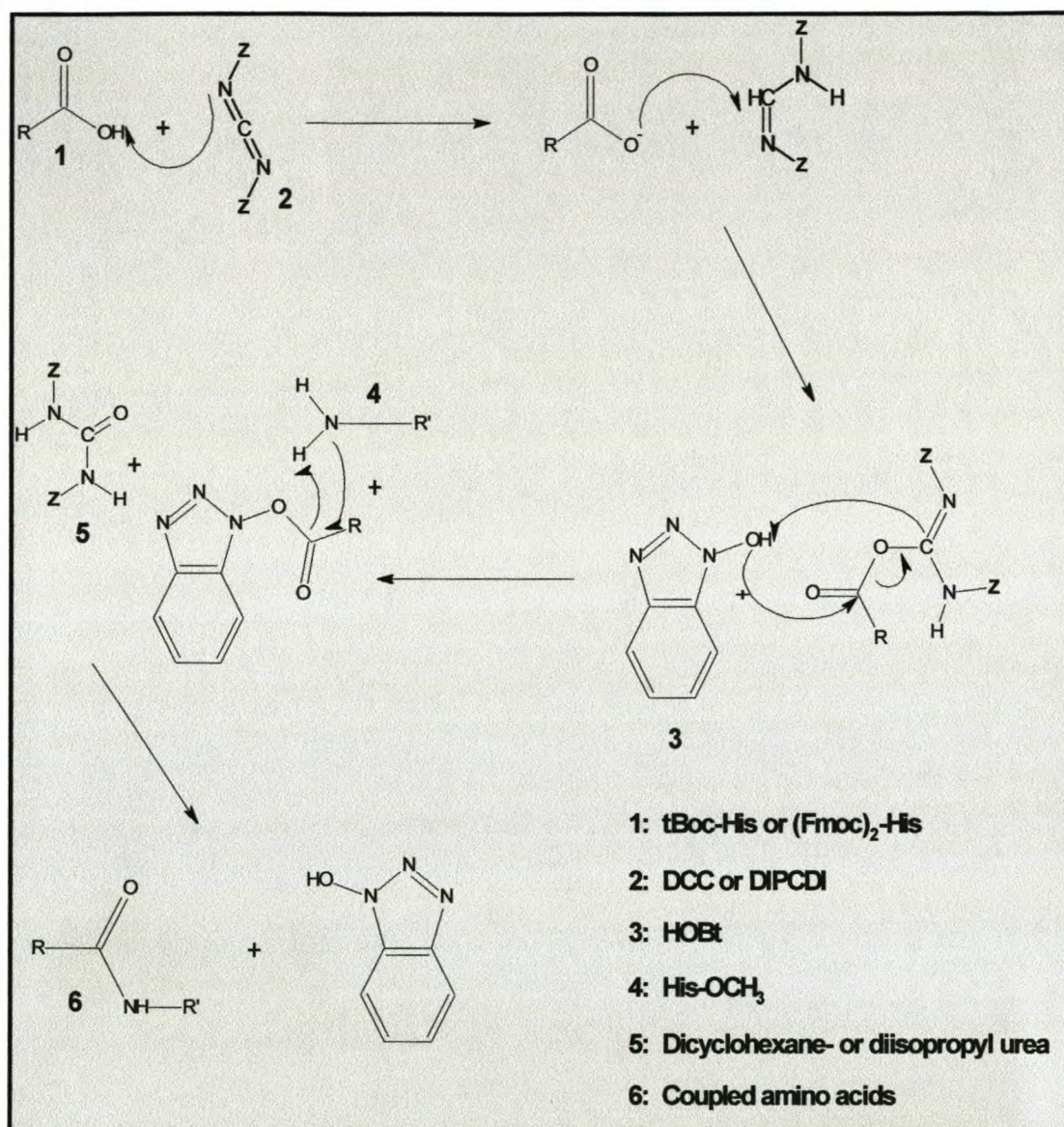


Figure 2.1.5: Schematic representation of the peptide bond formation using the dehydrating agents DCC or DIPCDI and the trapping agent HOBT.[67]

An alternative method was investigated using diethoxyphosphoryl cyanide[69;70] as a coupling agent (see Fig. 2.1.6) with the two amino acids $t\text{BOC-His}$ and $\text{His-OCH}_3 \cdot 2\text{HCl}$ and triethylamine (TEA) as base. This method was again characterised by difficulties in separating and cleaning of intermediates and low yields.

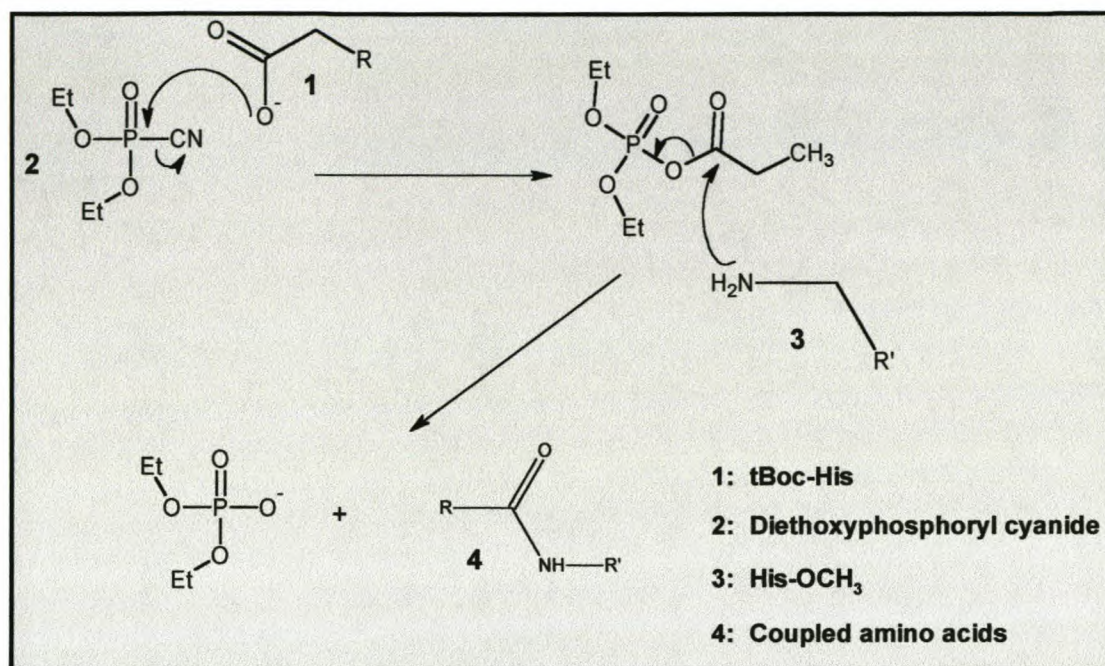


Figure 2.1.6: Schematic representation of the peptide bond formation using diethoxyphosphoryl cyanide as coupling agent.

The methods described in Section 3.5.5. and 3.5.6. were optimised from experience gained from the first two methods mentioned. It uses the same starting compounds as first mentioned method except that DCC was replaced with DIPCDI and DIPEA with TEA. This method, once it was optimised, proved to be fairly simple and straightforward and the synthesis can be completed within two days, working with relatively large quantities of starting compounds (1 – 2 g of amino acids). The yields are also favourable. Furthermore, it can be applied to synthesise His3 on the same scale.

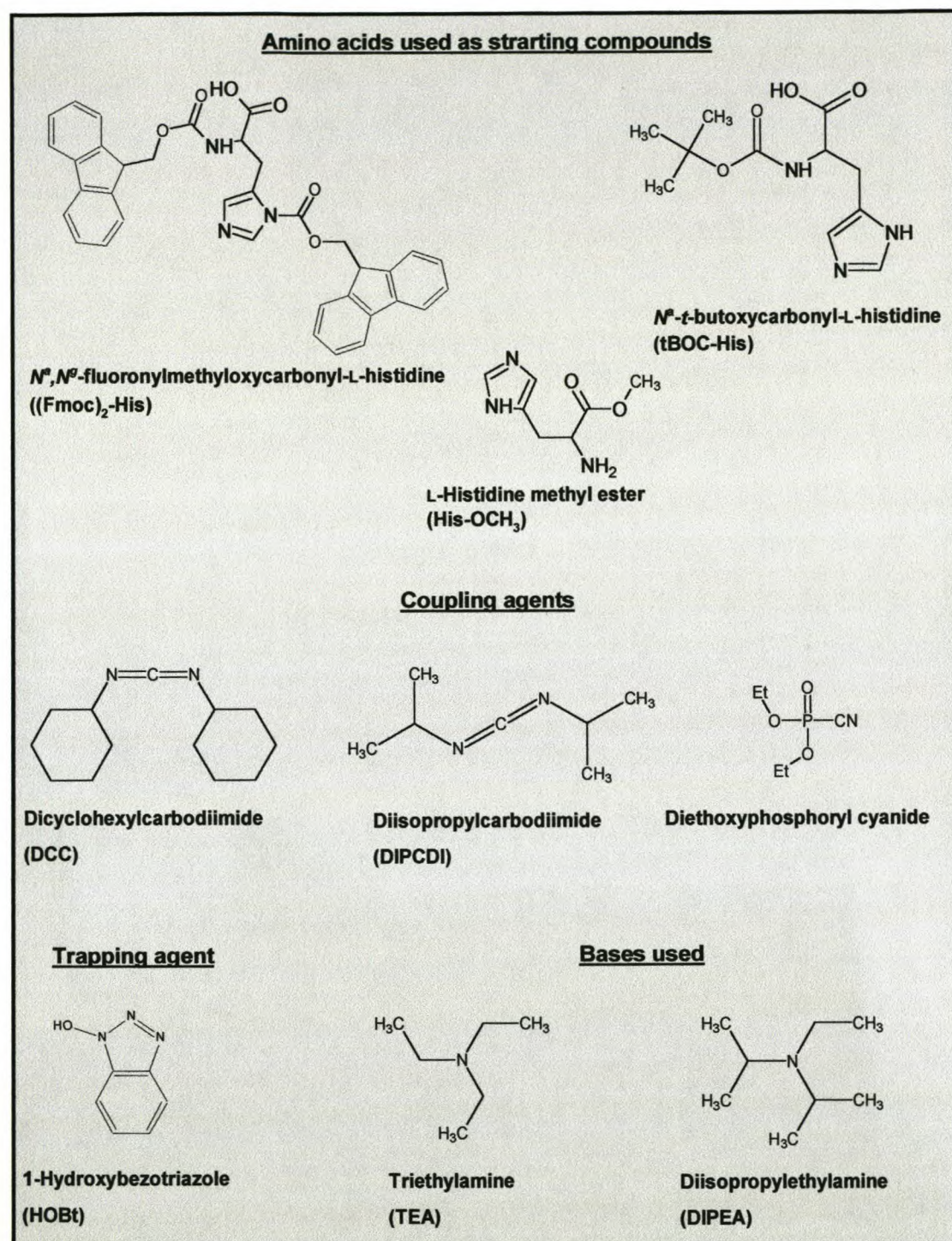


Figure 2.1.7: Reagents used during peptide synthesis.

2.2. Model complexes.

In this study nickel(II) and copper(II) ions were used to prepare the model complexes. These metal ions are borderline Lewis acids, and it is for this reason that they are the most commonly used in IMAC. The nitrogen atoms in the histidine side chains are also borderline Lewis bases in character.[71]

It was mentioned earlier that there should be at least one vacant co-ordination site on the metal ion, after coordination with the immobilising ligand, for interaction with the bio-molecule. Crystal structures of the model complexes *dimethyl N,N'-dicarboxymethyl-3,6-diazaoctanedioate copper(II) complex* (CuDMDDO) and *diethyl-N,N'-dicarboxymethyl-3,6-diazaoctanedioate diimidazole nickel(II) complex* (NiDEDDO(Im)₂) (see Chapter 4.2), clearly show such sites. In the copper complex the "vacant" site is the one occupied by the coordinated water molecule and in the nickel complex the two imidazoles indicates the potential sites, as it models the imidazole group of histidine.

Diethyl N,N'-dicarboxymethyl-3,6-diazaoctanedioate copper(II) complex (CuDEDDO) was synthesised and yielded blue crystals, like CuDMDDO, but afforded a poor crystal structure due to twinning.

Dimethyl and diethyl -N,N'-dicarboxymethyl-3,6-diazaoctanedioate nickel(II) complexes (NiDMDDO and NiDEDDO) and *dimethyl-N,N'-dicarboxymethyl-3,6-diazaoctanedioate diimidazole nickel(II) complex* (NiDMDDO(Im)₂) were synthesised. Suitable crystals for X-ray crystallography could not be obtained from the light blue precipitate of these complexes.

Slow crystallisation techniques such as slow evaporation of the solvent, crystallisation at low temperatures, addition of less polar solvents and layering were attempted to crystallise the complexes. None of these techniques yielded crystals.

Nickel and copper complexes of ethylenediaminediacetic acid (NiEDDA and CuEDDA) were synthesised as Infrared spectroscopy (IR) reference material to the

preceding complexes. EDDA is similar to the model ligands except for the methyl or ethyl carboxymethyl ester functions, which are absent (see Chapter 4.3.).

His2 and His3 were also reacted with the model complexes CuDMDDO and *dimethyl N,N'-dicarboxymethyl-3,6-diazaoctanedioate nickel(II) complex* (NiDMDDO). There was a definite change in colour, from blue to blue – purple, after the di- and tri-peptides were added, which indicated that there was interaction between the metal ion and the model peptides but no crystallisation took place. Samples of these complexes in solution were subjected to ES-MS analysis to gain extra information from the fragmentation pattern. The fragmentation pattern of His2 and His3 interacting with the complexes were expected to be different from these peptides on their own and to give insight in to the number and identity of the histidine residues taking part in the coordination with the metal ion. The ES-MS spectra of these samples were very complex and no definite conclusions could be made. This could be further investigated by altering the cone voltages and the detection modes of the ES-MS. Valuable information might also be gained from UV-VIS spectroscopy.

2.3. Metal binding capabilities of the ligand modified Pluronic.

UV-VIS spectroscopy was used to qualitatively determine whether the ligand-modified-Pluronic chelates metal ions. An excess of insoluble, basic copper carbonate [$\text{CuCO}_3 \cdot \text{Cu}(\text{OH})_2$] was added to aqueous solutions of the modified Pluronic, unmodified Pluronic and DMDDO. The Cu^{2+} in the salt is liberated by the reaction of the acidic protons in the ligand. The unreacted basic copper carbonate was filtered off, the filtrate diluted to the required concentration and the UV-VIS spectra of the three different solutions compared. All the solutions were made up in deionised (Milli-Q) water (see Chapters 3.7. and 4.5.).

When the unmodified Pluronic solution was made up to the same concentrations as that of the model ligand and model complex, it gave very low absorbancies ($1 \cdot 10^{-3}$). For model ligand and model complex solutions, however, absorbance readings went off the scale (>6) when made up to the same concentration as that of the Pluronic compounds. The different solutions were therefore made up at different concentrations. This enabled easier visual comparison and quantitative information can still be gained from the absorptivity values for the compounds.

Absorptivity (a) ($\text{cm}^{-1} \text{g}^{-1}$) was chosen above molar absorptivity (ϵ) ($\text{cm}^{-1} \text{mol}^{-1}$) as unit to work in. Pluronic has an average molecular weight (14600 Da), which makes it more precise to work with grams rather than moles. Beer's law was thus used in the $A = abc$ form with (A) being absorbance, (a) absorptivity in $\text{cm}^{-1} \text{g}^{-1}$, (b) path length in cm and (c) concentration in $\text{g} \text{l}^{-1}$. [72]

Other attempts in determining the metal binding capabilities of ligand-modified-Pluronic.

The initial experiments to determine the metal chelating abilities of the ligand-modified-Pluronic were aimed to be quantitative. The amount of metal ion (Cu^{2+}) chelated would be determined by mass balance calculations of the amount of copper removed from a known concentration copper solution and also determining the amount of copper ions that are chelated by the modified Pluronic, by protonating the

ligands, with a strong acid like HCl, and thus releasing the copper ions into solution. Concentrations were determined by means of Inductive Coupled Plasma Mass Spectrometry (ICP-MS).

In initial experiments 1 cm² pieces of flat sheet polysulphone membrane were coated with ligand-modified-Pluronic and unmodified Pluronic. The coated membrane squares were then treated with a NaOH solution to deprotonate the ligand groups after which it were treated with a known copper solution and then with an acid solution. The squares were rinsed with deionised (Milli-Q) water between every step. Every procedure was done in duplicate. Uncoated membrane pieces were also subjected to the same procedure to act as a standard and also check for non-specific adsorption of the copper ions onto the membrane surface. The concentration changes in the known copper solution and the acid solution was too small to be detected by ICP-MS.

Larger (100 and 500 cm²) pieces of membrane were then used and subjected to the same procedures. Here concentration changes were observed, but the values were inconsistent between duplicates and inconclusive. This was due to practical problems like inconsistent membrane coverage on the paper support and the membrane rolling up allowing for uneven circulation of the copper solution over the membrane surface.

It was decided to conduct similar experiments on hollow fibre polysulphone membranes. The fibres have an internal diameter of 0,07 cm, a length of 25 cm and 150 were bundled together. This gave a very large internal surface area of $8,25 \cdot 10^2$ cm². The bundle was mounted in a Perspex reactor fitted with an inlet and outlet. This membrane reactor was placed in a closed system where a solution could be pumped through the membranes by means of a peristaltic pump.

The first step was to ascertain how much unmodified Pluronic is adsorbed onto the membrane surface. A Pluronic (5g/l) solution was pumped through the membranes for 6 h after which it was rinsed with deionised water. The stripping solution (3:2 hexane:isopropanol), used to strip Pluronic from the membrane surface, degraded the Perspex housing of the membrane matrix. Experiments could not be continued due to time restraints as a new membrane matrix would have to be made and a suitable stripping solution will have to be found.

Coating concentration and adsorption isotherms for Pluronic and the stripping solution was recommended by fellow students working on a related project on determining the adsorption characteristics of Pluronic onto flat-sheet polysulphone membranes.[73]

It was also during this time that the RF source of ICP-MS became dysfunctional and could not be repaired in time to continue these types of experiments.

As an alternative crude polysulphone beads (used for making polysulphone membranes) were investigated as a solid support. The beads have an average diameter of *ca.* 0,26 cm. The beads (75 g) were tightly packed in a column yielding a total surface area of *ca.* $1,5 \cdot 10^3 \text{ cm}^2$. The column was integrated into a closed system similar to the one used above. A conductivity meter fitted with a double wall flow-through-cell electrode was used for the detection of changes in Cu^{2+} concentration.

Solutions were pumped from a double wall reaction flask through the column, from there through the flow-through-cell detector and back into the reaction flask. The flask and the cell were kept at a constant temperature (25°C) by means of water circulating from a temperature controlled water bath, through the double walls. The conductivity meter was calibrated in the expected conductivity range by means of standard solutions made up to the specifications indicated by the manufacturer.

The beads were coated by covering them with the Pluronic solutions for at least 24 h, after which they were filtered and rinsed with deionised water and dried before packing them into the column.

A fixed volume (50 ml) of water was placed in the reactor flask and pumped through the system until all the air was removed and the conductivity meter stabilised. A CuNO_3 solutions was added in small increments (*ca.* 0,3 ppm; 0,5 ml), using a burett, to the solution in the flask. After every addition the solution was circulated until the conductivity reading stabilised after which the circulation was stopped and the reading was taken once it became completely stable. This is very important since temperature

has a great influence on conductivity and by stopping the circulation the solution in the electrode had time to adjust to the same temperature (25°C) for every reading.

The Cu²⁺ retention was tested for the following systems:

1. Clean beads,
2. Beads treated with a Pluronic solution (5 g/l),
3. Beads treated with a Pluronic (5 g/l) and NaOH solution,
4. Beads treated with a ligand-modified-Pluronic (5 g/l) solution and
5. Beads treated with a ligand-modified-Pluronic (5 g/l) and NaOH solution

Conductivity (μS) vs. concentration (ppm) standard curves were plotted for the respective conductivity regions. Conductivity readings after every titration was inserted into the linear equation of the relevant standard curve and the concentration (ppm) for that point calculated. This calculated concentration value was plotted against the corresponding conductivity value.

The aim of the experiment was to obtain a breakthrough value where the ligand-modified-Pluronic became saturated with copper ions and a sudden rise in conductivity would indicate an excess of copper in the solution. This did not happen, since all the plots were linear. This indicated that there was no sudden rise in conductivity which would be indicated by a step in the graph.

The reason for this is probably insufficient coating of the beads taking place or desorption of the Pluronic molecules during the experiment. The surface characteristics of the beads are probably not the same as that of the membrane's surface. The physical and chemical characteristics of polysulphone can change when it is dissolved and cast into membranes together with other additives.

The last alternative, due to time constraints, to prove that the ligand-modified-Pluronic did indeed bind metal ions was in solution by means of UV-VIS spectroscopy as described in the beginning of this section.

Chapter 3: Experimental.

3.1. Reagents

Ethylenediaminetetraacetic dianhydride (98%), L-histidine methyl ester dihydrochloride (97%) ethylenediamine-*N,N'*-diacetic acid (>98%) and sodium hydride (55 - 65% in oil suspension) were supplied by Aldrich SA. Fluka supplied *N*^α-tBoc-L-histidine (> 99%) and 1-hydroxybenzotriazole (> 98%).

Diisopropylcarbodiimide was supplied by Milli Gen. Triethylamine (>99%), diethyleneglycol monomethyl ether (98%) and trifluoroacetic acid (spectroscopic grade) were supplied by Merck. Saarchem SA supplied nickel chloride (AR grade), nickel carbonate, basic cupric carbonate and sodium hydroxide (min. 98%).

Imidazole was supplied by ICN – Biochemicals (distributed by Separations) and Pluronic[®] F108 by BASF.

Diethyleneglycol monomethyl ether (DEGM) was dried by means of a benzene azeotrope after which it was distilled under a dry nitrogen atmosphere onto 3Å molecular sieves. It was also stored under nitrogen.

Sodium hydride was cleaned by washing it four times with dry pentane under a nitrogen atmosphere. It was also stored and handled under nitrogen.

3.2. Solvents

Dimethyl formamide (99,5%, BDH Chemicals) was dried over KOH (10 – 20 g/L) for at least 12 h to remove residual water, after which it was distilled at reduced pressure (10 – 18 mbar) at 60°C under a dry argon atmosphere. The first 10% of the distillate was discarded. The distilled DMF was kept in dark bottles.

Pure DMF is especially important when used in peptide chemistry using Fmoc protecting group as contaminants like secondary amines and water can liberate the Fmoc protecting groups prematurely during synthesis. Water can also react with DMF to form secondary amines [which were tested for through the Sanger's test for

amines (see Chapter 3.4)] and formic acid:[68] $(\text{CH}_3)_2\text{NCOH} + \text{H}_2\text{O} \rightarrow (\text{CH}_3)_2\text{NH} + \text{HCOOH}$.

Ethanol (99,8%, Merck) and methanol (99,5%, Kimix) was dried 0,5 l at a time. About 2 g magnesium turnings were reacted with 100 ml of the alcohol and iodine under a dry nitrogen atmosphere. The mixture was stirred continuously and slightly heated. Iodine was added until all of the magnesium turnings reacted, after which the rest of the alcohol (400 ml) was added to the mixture and stirred for another hour. The alcohol was then distilled under a dry nitrogen atmosphere onto 3Å molecular sieves and stored under nitrogen.[74]

Ethyl acetate (99,5%, BDH Chemicals) was used without further drying.

Diethyl ether (AR, Kimix) and tetrahydrofurane (THF) (AR, Kimix) were dried over KOH flakes for at least 24 hours and distilled under an N₂ atmosphere. Toluene (AR, Kimix) was dried over 3Å molecular sieves for at least 24 hours and distilled under a N₂ atmosphere.

Distilled water was used for the synthesis of the metal complexes and deionised (Milli-Q) water for UV/VIS spectroscopy.

Dimethyl sulfoxide-*d*₆ (DMSO-*d*₆; 99,9%; Aldrich) and tetramethylsilane (TMS; 99,9%; Aldrich) were used as NMR solvent and internal standard respectively.

3.3. Physical measurements.

NMR: The Pluronic and modified Pluronic spectra were recorded on a Varian Inovo 600 MHz spectrometer with a $D_1 = 1$ pulse delay of 1 s, for the ^{13}C spectra recorded over an 8 h period. All the other spectra were recorded on a Varian VXR 300 MHz spectrometer.

X-ray diffraction: Crystal data were obtained on a Nonius Kappa CCD diffractometer fitted with an area detector.

Infrared spectroscopy: IR spectra were measured on a Perkin-Elmer 1720 Fourier Transform Infrared spectrometer. Spectroscopic grade KBr powder (stored under N_2 atmosphere) was used to press the pellets in a glove-box purged with N_2 . The sample compartment was also purged with dry air from a Perkin-Elmer circulatory air dryer. Every evening the air dryer was set to regenerate to ensure that hardly any water vapour or CO_2 can interfere with the measurements.

Mass spectrometry: The model ligands, His2 and His3 and the crude product mixtures of the reactions describe in section 3.5.3. were analysed by a Micro-Mass Quattro, triple quadrupole mass spectrometer fitted with electrospray ionisation.

UV/VIS spectroscopy: Ultra violet and visible light spectra were recorded on a GBC UV/VIS 920 spectrometer using 1 cm quartz cuvettes. Solutions were made up with deionised (Milli-Q) water and water was also used as blanks.

Thin layer chromatography (TLC) was performed on Alugram[®] SIL G/UV₂₅₄ (Macherey – Nagel) plates coated with silica gel 60 and fluorescent indicator UV₂₅₄.

3.4. Tests for free amino groups and amines.

The Kaiser test for free amino groups requires three solutions: (a) 500 mg of ninhydrin in 10 ml of 95% ethanol, (b) 40 mg of phenol in 10 ml of 95% ethanol and (c) 2 ml of a 0,001 M KCN solution diluted to 100 ml with distilled pyridine. The sample was placed in a small test tube and the excess DMF and DIPEA evaporated by means of a nitrogen stream. Four drops of each of the solutions were added to the sample and it was placed in a water bath at 80°C for 5 min. A positive test is indicated when the colour changes to blue.

The Sanger's test for amines [68] was applied to the DMF used for peptide synthesis involving the use of Fmoc protected histidine to test for the presence of secondary amines. The test was carried out by mixing equal volumes of 1-fluoro-2,4-dinitrobenzene (FDNB)(1,0 mg/ml FDNB in 95 % ethanol) and DMF. This mixture was left at room temperature for 30 min. The absorbance of the mixture was determined at 381 nm and 0,5 mg/ml was used as blank, which had an absorbance in the region of 0,2. Suitably pure DMF had an absorbance of not more than 0,07 units higher than that of the blank.

3.5. Synthesis of the model ligands.

3.5.1. Diethyl *N,N'*-dicarboxymethyl-3,6-diazaoctanedioate (DEDDO).

Analytical results are shown in Chapter 4.

Ethylenediaminetetraacetic dianhydride (5,00 g; 20 mmol) was mixed with 100 ml of ethanol and refluxed for 6 hours. This solution was filtered while hot and the ethanol was removed under reduced pressure until a sticky light brown residue remained. 50 ml of ethyl acetate was added to this and it was brought to reflux. The resultant solution was left in a freezer for 8 h, after which the white crystals that formed were filtered, washed with ether and dried under high vacuum. *Diethyl N,N'*-dicarboxymethyl-3,6-diazaoctanedioate was obtained in 5,92g (85%) yield and was characterised by NMR, IR, ES-MS and EI-MS.

3.5.2. Dimethyl *N,N'*-dicarboxymethyl-3,6-diazaoctanedioate (DMDDO).

The same procedure was used at the same scale as with DEDDO (3.5.1), but methanol was used instead of ethanol. *Dimethyl N,N'*-dicarboxymethyl-3,6-diazaoctanedioate was obtained in 6,27g (98%) yield and was characterised by NMR, IR, ES-MS and EI-MS.

3.5.3. Model reactions for determining the reaction conditions and reagent addition sequence to couple the ligand to Pluronic[®] F108.

The following four procedures are key-points in the process of determining the reaction conditions for coupling the ligand to Pluronic. As mentioned in Chapter 2.1. it was very difficult to separate the desired product from the by-product. As a result of this the final product mixtures were never fully characterised except for ES-MS, which was used to roughly estimate the quantities of the different components in the crude product mixture.

First procedure: The sodium salt of DEGM was prepared by dissolving DEGM (1,202 g; 1,178 ml; 10 mmol) in dried THF (15 ml) and adding NaH (240 mg; 10 mmol) to it, after which it was stirred under nitrogen in an ice bath until gas evolution ceased. Ethylenediaminetetraacetic dianhydride (2,562 g; 10 mmol) was dissolved in dried DMF (20 ml) at 80°C and then cooled down to 40°C. The THF solution was added drop-wise to the DMF solution under nitrogen. Once all the DEGM salt solution was added to the DMF solution the THF was evaporated under reduced pressure and the resultant mixture was stirred for 3 h at 40°C. After this time the DMF was evaporated under reduced pressure and the remaining residue redissolved in 20 ml of dried methanol and heated under reflux conditions for another 3 h, after which the methanol was evaporated under reduced pressure to dryness. A sample of the crude product mixture was sent for ES-MS analysis.

Second procedure: Ethylenediaminetetraacetic dianhydride (2,562 g; 10 mmol) was dissolved in dried DMF (20 ml) at 80°C under nitrogen. DEGM (601 mg; 589 µl; 5 mmol) was dissolved in dried DMF (3 ml) and slowly added to the dianhydride solution. This mixture was stirred at this temperature for 3 h, after which the DMF was evaporated under reduced pressure. The remaining residue was dissolved in dried methanol (20 ml) and heated under reflux conditions for another 3 h after which time the methanol was evaporated under reduced pressure. A sample of the crude product mixture was sent for ES-MS analysis.

Third procedure: The sodium salt of DEGM was prepared by dissolving DEGM (300 mg; 294 µl; 2,5 mmol) in dried THF (15 ml) and adding NaH (60 mg; 2,5 mmol) to it after which it was stirred under nitrogen in an ice bath until gas evolution ceased. The volume of the THF was reduced to ca 3 ml and dry DMF (ca 15 ml) was added to this. Ethylenediaminetetraacetic dianhydride (641 mg; 2,5 mmol) together with imidazole (340 mg; 5 mmol) was dissolved in dried DMF (10 ml) at 50°C. The salt solution was added drop-wise to the dianhydride solution and the resultant stirred at this temperature for 2 h after which dried methanol (7 ml) was added and it was stirred at the same temperature for another 2 h. All the solvent was evaporated under reduced pressure and the crude product mixture was sent for ES-MS analysis.

Fourth procedure: Ethylenediaminetetraacetic dianhydride (641 mg; 2,5 mmol) together with imidazole (340 mg; 5 mmol) was dissolved in dried DMF (20 ml) at 40°C under nitrogen. DEGM (300 mg; 294 µl; 2,5 mmol) was dissolved in dried DMF (3 ml) and added drop-wise to the dianhydride solution. This mixture was stirred (at 40°C) for 3 h after which dried methanol (1 ml) was added and it was stirred for another 3 h. All the solvent was evaporated under reduced pressure and a sample of the crude product mixture was sent for ES-MS analysis.

3.5.4. Bis[2-(2-methoxyethoxy)ethyl] *N,N'*-dicarboxymethyl-3,6-diazaoctanedioate (BMDDO).

Ethylenediaminetetraacetic dianhydride (1,281 g; 5,0 mmol) was dissolved in 20 ml DMF at 80°C. An excess (5 ml; 43 mmol) of diethyleneglycolmonomethylether (DEGM) was added and the mixture was stirred at this temperature for 4 hours, after which the DMF was evaporated under reduced pressure. The oily residue was redissolved in a minimum of methanol and ether was added until an amorphous product separated out. The excess solvent was removed by means of a pipette and then under vacuum. This procedure was repeated three times. The final product was dried under high vacuum for 15 hours to yield *bis*[2-(2-(methoxyethoxy)ethyl)] *N,N'*-dicarboxymethyl-3,6-diazaoctanedioate as a viscous, light brown oil, in a yield of 2,45g (93%) which was characterised by NMR.

3.5.5. *L*-Histidyl-*L*-histidine methylester (His2).

N^α-*t*Boc-*L*-histidine (1,024 g; 4,0 mmol) was dissolved in 50 ml DMF, by stirring the mixture overnight at room temperature. *L*-Histidine methyl ester dihydrochloride (0,968 g; 4,0 mmol) and triethylamine (1,109 ml; 8,0 mmol) was dissolved in 50 ml of DMF in the same way. The volume of these solutions were reduced to 20 ml each under reduced pressure, they were combined and diisopropylcarbodiimide (DIPCDI) (0,752 ml, 4,8 mmol) and 1-hydroxybenzotriazole (HOBT) (0,649 g; 4,8 mmol) were added. This mixture was stirred for 48 hours, after which the DMF was removed under reduced pressure. During this process diisopropyl urea started to crystallise out as the volume became less. These crystals were filtered off and washed with DMF

before the evaporation process was continued. These steps were repeated at least three times to remove most of the urea. All the solvent was evaporated and the residue was dissolved in a minimum of methanol.

The methanol solution was adsorbed onto ca 2 g silica gel (Kieselgel 60) by evaporating the methanol to dryness under vacuum.

Separation of the product, N^α-tBOC-L-histidyl-L-histidine methyl ester, from the by-products (diisopropyl urea) and unreacted compounds (HOBt) was investigated by means of thin layer chromatography. The following results were obtained with a 1:2 ethanol/ethyl acetate eluant.

	Compound	Rf – Value	Reaction with I ₂	Fluorescence
1	HOBt	0,85	Weak	Strong
2	Product	0,14	Strong	Weak
3	Urea	0,04	Weak	Very weak

The components were separated on 15 cm x 2,5 cm diameter flash chromatography, silica gel column. The column was packed and the silica (Kieselgel 60) with the adsorbed compounds was brought onto the column and eluted with a 1:2 ethanol/ethyl acetate mixture until the HOBt appeared. A 1:1 ethanol/ethyl acetate eluant was used to separate the product fraction. Ethanol was employed to separate the last part of the product from the urea. The compounds were collected in 25 ml fractions.

The product fractions were combined and the eluant was removed under reduced pressure yielding crude t-Boc(His)₂. The residue was treated with 3 ml of a 95% trifluoro acetic acid solution for 1 hour at room temperature, after which the acid was removed under reduced pressure for 15 h. The product was redissolved in a small amount of methanol and reprecipitated, by pouring 30 ml ice-cold ether onto the methanolic solution. A fine white powder resulted. A centrifuge was used to separate and clean the final product. It was washed 3 times with ether and dried overnight in a freeze-dryer to yield L-histidyl-L-histidine methyl ester (His₂) in 0.98g (80%) yield. Characterised by NMR and ES-MS.

3.5.6. L-Histidyl-L-histidyl-L-histidine methyl ester (His3)

His2 (0,919 g; 3,0 mmol) was dissolved in 50 ml of DMF, by stirring the mixture at room temperature for 15 hours. N α -t-Boc-L-histidine (0,766 g; 3,0 mmol) was dissolved in 50 ml of DMF in the same way. The volume of these solutions was then reduced to 20 ml under reduced pressure, they were combined and diisopropylcarbodiimide (DIPCDI) (0,517 ml, 3,3 mmol) and 1-hydroxybenzotriazole (HOBt) (0,446 g; 3,3 mmol) were added. This mixture was stirred for 48 hours, after which the DMF was removed under reduced pressure. During this process diisopropyl urea started to crystallise out as the volume became less. These crystals were filtered off and washed with DMF before the evaporation process was continued. These steps were repeated at least three times to remove most of the urea. When all the DMF was evaporated the residue was dissolved in a minimum of methanol.

The product in the methanolic solution was adsorbed onto ca 2 g silica gel (Kieselgel 60) by evaporating the methanol to dryness under reduced pressure.

Separation of the product, N α -tBoc-L-histidyl-L-histidyl-L-histidine methyl ester, from the by-products (diisopropyl urea) and unreacted compounds (HOBt) was investigated by means of thin layer chromatography. The following results were obtained with a 1:2 ethanol/ethyl acetate eluant.

	Compound	Rf – Value	Reaction with I ₂	Fluorescence
1	HOBt	0,85	Weak	Strong
2	Urea	0,08	Weak	Very weak
3	Product	0,01	Strong	Weak

The components were separated on 15 cm x 2,5 cm diameter flash chromatography, silica gel column. The column was packed and the silica with the adsorbed compounds were brought onto the column and eluted with a 1:2 ethanol/ethyl acetate mixture until the HOBt appeared. A 2:1 ethanol/ethyl acetate eluant was used to separate the urea fraction and methanol was used to strip the product from the column. The compounds were collected in 25 ml fractions.

The product fractions were combined and the eluant removed under reduced pressure. The residue was treated with 3ml of a 95% trifluoro acetic acid solution for 1 hour at room temperature, after which the acid was removed under high vacuum over a period of 15 hours. The product was dissolved in a small amount of methanol and precipitated by pouring 30 ml ice-cold ether onto the methanolic solution. A fine white powder resulted and a centrifuge was used to separate and clean the final product. The product was washed 3 times with ether and dried overnight in a freeze-dryer to yield L-histidyl-L-histidyl-L-histidine methyl ester (His3) in 1,01g (76%) yield. Characterised by NMR and ES-MS.

3.6. Synthesis of the model complexes.

3.6.1. Diethyl- and dimethyl *N,N'*-dicarboxymethyl-3,6-diazaoctanedioate copper(II) complex (CuDEDDO and CuDMDDO respectively).

Syntheses of these two complexes are the same. The synthesis for CuDMDDO is described below:

DMDDO (1,00 g; 3,1 mmol) was dissolved in 5 ml distilled water at 60°C. Basic copper carbonate, $\text{CuCO}_3\text{Cu}(\text{OH})_2$ (238 mg; 1,6 mmol), was added to the DMDDO solution and stirred at this temperature until all of the basic copper carbonate dissolved and evolution of gaseous CO_2 ceased. This solution was left to stand overnight during which time deep blue crystals formed. The crystals were filtered and washed with cold ethanol to yield *dimethyl N,N'*-dicarboxymethyl-3,6-diazaoctanedioate copper(II) complex 1,05 g (89%). Characterised by X-ray crystal structure, IR, EI-MS and ES-MS.

Synthesis of CuDEDDO is identical, starting from DEDDO (1,08g; 3,1 mmol), 5 ml of distilled water and $\text{CuCO}_3\text{Cu}(\text{OH})_2$ (238 mg; 1,6 mmol) yielding 0,67 g (53%) CuDEDDO. Characterised by IR, EI-MS and ES-MS.

3.6.2. Diethyl- and dimethyl *N,N'*-dicarboxymethyl-3,6-diazaoctanedioate nickel(II) complex (NiDEDDO and NiDMDDO).

The syntheses of the two complexes were the same. The synthesis for NiDMDDO is described below. Nickel chloride ($\text{NiCl}_2 \cdot 6\text{H}_2\text{O}$) and nickel carbonate (NiCO_3) were considered as possible starting compounds.

The nickel chloride route: DMDDO (1,00 g; 3,1 mmol) and NaOH (248 mg; 6,2 mmol) were dissolved in 5 ml distilled water at 60°C. $\text{NiCl}_2 \cdot 6\text{H}_2\text{O}$ (737 mg; 3,1 mmol) was added to the ligand solution and stirred at this temperature for 30 min, after which it was left to stand overnight at room temperature. A fine, light blue precipitate formed which was filtered and washed with a small amount of ice cold

water. The precipitate was dissolved in a little hot water to form a saturated solution, which was left to stand at room temperature for 48 hours. Once again a fine, light blue precipitate formed which was filtered and washed with cold ethanol to yield 0,45 g (39%) *dimethyl N,N'-dicarboxymethyl-3,6-diazaoctanedioate nickel(II) complex*. Characterised by IR, EI-MS and ES-MS.

The nickel carbonate route: DMDDO (1,00 g; 3,1 mmol) was dissolved in 5 ml distilled water at 60°C, NiCO₃ (356 mg, 3,1 mmol) was then added and stirred at this temperature until all the NiCO₃ had dissolved and CO₂ gas evolution seized. Again a fine, light blue precipitate formed when the solution was left to stand at room temperature. This precipitate was then treated in the same way as the preceding nickel chloride route to yield 0,26 g (22%) *dimethyl N,N'-dicarboxymethyl-3,6-diazaoctanedioate nickel(II) complex*.

The synthesis of NiEDDO is identical, starting from DEDDO (1,08 g; 3,1 mmol), 5 ml of distilled water, NaOH (248 mg; 6,2 mmol) and NiCl₂·6H₂O (737 mg; 3,1 mmol) also yielding a light blue precipitate NiEDDO in 0,61 g (48%) yield. Characterised by IR, EI-MS and ES-MS.

3.6.3. Ethylenediaminediacetic *N,N'*-diacetato nickel(II) and copper(II) complexes (NiEDDA and CuEDDA).

The synthesis of NiEDDA and CuEDDA was taken from Averill *et al.*[75].

NiEDDA: EDDA (250 mg; 142 mmol) and NaOH (114 mg; 284 mmol) were dissolved in ca 10 ml of distilled water and heated to 80°C. To this was added NiCl₂·6H₂O (371 mg; 156 mmol) and stirred for 15 min at 80°C, after the mixture was left to cool and stand for 12 h. The blue crystals that formed was filtered off and washed with 5 ml of ethanol. The crystals was redissolved in a minimum amount of distilled water and again left to crystallise for 12 h. Again the crystals were filtered and washed with ethanol and left to dry in air to obtain ethylenediaminediacetic *N,N'*-diacetato nickel(II) complex in 183 mg (56%) yield. Characterised by IR, EI-MS and ES-MS.

CuEDDA: EDDA (250 mg; 142 mmol) was suspended in ca 10 ml distilled water at 80°C. $\text{CuCO}_3\text{Cu}(\text{OH})_2$ (250 mg; 142 mmol) was added to this and stirred at this temperature until the evolution of gaseous CO_2 ceased. The mixture was filtered and left to cool at room temperature for 12 h after which time dark blue crystals form. These were filtered off and washed with 5 ml ethanol. The product was recrystallised from a minimum amount of distilled water filtered and washed with ethanol and left to dry in air to obtain ethylenediaminediacetic *N,N'*-diacetato copper(II) complex in 206 mg (61%) yield. Characterised by IR, EI-MS and ES-MS.

3.6.4. Diethyl *N,N'*-dicarboxymethyl-3,6-diazaoctanedioate di-imidazole nickel(II) complex (NiDEDDO(Im)₂)

DMDDO (1,00 g; 2,9 mmol) and NaOH (230 mg; 5,7 mmol) were dissolved in 5 ml distilled water at 60°C. $\text{NiCl}_2 \cdot 6\text{H}_2\text{O}$ (683 mg; 2,9 mmol) was added to the ligand solution and stirred for 30 min., after which imidazole (391 mg; 5,7 mmol) was added. Shortly after the addition of the imidazole, small crystals started to form. Distilled water was added until all the crystals dissolved again. The solution was stirred for another 15 min at 60°C and then left to stand at room temperature for 24 hours. The light blue crystals that formed were filtered and washed with cold ethanol to obtain *diethyl-N,N'*-dicarboxymethyl-3,6-diazaoctanedioate diimidazole nickel(II) complex in a 860 mg (58%) yield. Characterised by X-ray crystal structure, IR, EI-MS and ES-MS.

3.7. Modification of the terminal hydroxy end groups of Pluronic[®] F108 to methyl Pluronic mixed ester of *N,N'*-dicarboxymethyl-3,6-diazaoctanedioic acid.

Every step in this procedure was performed under an inert and dry atmosphere.

Pluronic (1,46 g; ~ 100 μ mol) was dried by applying a toluene/ethanol azeotrope mixture three times and precipitating the Pluronic with ether. After filtering it, the Pluronic was dried under high vacuum at room temperature for 2 hours after which it was dissolved in dried DMF (30 ml) and filtered through anhydrous MgSO_4 .

Ethylenediaminetetraacetic dianhydride (256 mg; 1,0 mmol) and imidazole (136 mg; 2,0 mmol) was dissolved in dried DMF (10 ml) that was filtered through MgSO_4 , at 30°C.

The Pluronic solution was very slowly added to the dianhydride solution at 30°C. After the addition of all the Pluronic, the resultant solution was concentrated to 15 ml by evaporating some of the DMF under reduced pressure. This mixture was stirred left overnight at 40°C, methanol (2 ml) was added and it was allowed to react for another 8 hours, after which all the DMF and excess methanol was removed under reduced pressure. The residue was treated with 80 ml toluene to selectively dissolve the modified Pluronic. The DMDDO by-product is insoluble in toluene and was filtered off. The toluene solution was concentrated to 30 ml and 100 ml ether was added to precipitate the modified Pluronic. The obtained product was filtered and dried under reduced pressure and yielded 1,47 g ligand-modified-Pluronic. Characterised by NMR and UV-VIS spectroscopy (see Chapter 4.5.).

3.8. UV-VIS spectroscopy.

All the solutions (see Table 3.7.1.) were made up in deionised (Milli-Q) water in volumetric flasks.

The model ligand DMDDO, the ligand modified Pluronic, and unmodified Pluronic was reacted with an excess of basic copper carbonate ($\text{CuCO}_3 \cdot \text{Cu}(\text{OH})_2$), which is insoluble in water, for two hours at 80°C . The excess basic copper carbonate was filtered of and the filtrate diluted to the desired concentration.

Table 3.7.1: The solutions and their concentrations used to record the UV-VIS spectra.

Type of solution	Concentration
DMDDO	$2,0 \cdot 10^{-4}$ M
Ligand modified Pluronic	0,6 g/L
Unmodified Pluronic	1,0 g/L
CuDMDDO	$1,0 \cdot 10^{-4}$ M (UV); $2,0 \cdot 10^{-3}$ M (VIS)
Cu^{2+} + Ligand modified Pluronic	0,25 g/L (UV); 5,0 g/L (VIS)
Cu^{2+} + Unmodified Pluronic	1,0 g/L (UV)
Water	Blank

See Table 4.5.1. for the absorptivity values of the solutions and their respective concentrations.

4. Results.

4.1. NMR Results.

Nuclear magnetic resonance (NMR) spectroscopy was instrumental in determining the structure of the ligand modified Pluronic. When modifying the end groups of such a large polymer, NMR is one of the few analytical techniques available to study the changes made. Yaniç *et al.*[76] characterised Pluronic by means of NMR. For this study it was necessary to make a series of model compounds to compare with that of the final product to verify a successful conversion.

Ligand modification of Pluronic was achieved in two steps. In the first step Pluronic was reacted with the one end of the dianhydride and in the second step methanol was reacted with the other side to yield the final product. It was therefore necessary to have model ligands that would simulate both sides of the reacted dianhydride. This justifies the DMDDO, DEDDO and BMDDO model compounds. It was also necessary to check for unreacted anhydride groups as well as possible side reactions like water, instead of methanol, reacting with the anhydride yielding the unwanted, pentadentate tri-carboxymethyl product. Thus the spectra of Pluronic, EDTA and the dianhydride were also needed for comparison.

^{13}C spectra proved to be more useful than the ^1H spectra when comparing the model ligands to that of Pluronic spectra. In the ^1H spectra Pluronic has a large footprint, caused by the PEO tethers that drowns the weak, ligand signals and makes it difficult to find suitable integration values. This effect was less pronounced in the ^{13}C spectra, where α (δ 60,40) and β (δ 73,09) carbons of Pluronic can be distinguished (see Table 4.1.7.)

Based on the chemical shift changes of these two carbons, it can be deduced that the ligand is attached to Pluronic (α δ = 62,96; β δ = 68,11). This shifting of the α and β carbons compares favourably with the α and β shifts in BMDDO (α δ = 63,27; β δ = 68,44). Also the difference between, the α and β carbons of BMDDO ($\Delta\delta$ ($\beta - \alpha$) = 5,17 ppm) and that of modified Pluronic ($\Delta\delta$ ($\beta - \alpha$) = 5,15 ppm) are similar (see

Tables 4.1.6. and 4.1.8.) Furthermore the DEGM ester (in BMDDO) and Pluronic ester (in the ligand modified Pluronic) carbonyl chemical shifts (Pluronic ester. $\delta = 171,80$; DEGM ester $\delta = 171,44$) are also very similar. Also similar is the shifts of the methyl ester carbonyls of DMDDO and that of the ligand modified Pluronic (Plu-MDDO $\delta = 171,76$; DMDDO $\delta = 171,20$). The acid carbonyls of DMDDO ($\delta = 172.21$), BMDDO ($\delta = 172.94$) and the modified Pluronic ($\delta = 172.78$), are also comparable. In modified Pluronic this peak shows a slight broadening due to the small difference in the chemical surroundings of the two acid carbonyls. There is also good correlation between the ethylenediamine carbon shifts of the model ligands and that of the modified Pluronic. The same applies for the carboxymethyl groups of the esters and acid groups, and the methyl group of the methyl ester. (Tables 4.1.1. to 4.1.8.)

Although the peak intensities of the modifications are very low, NMR still provides a powerful tool for resolving the structure of this huge molecule.

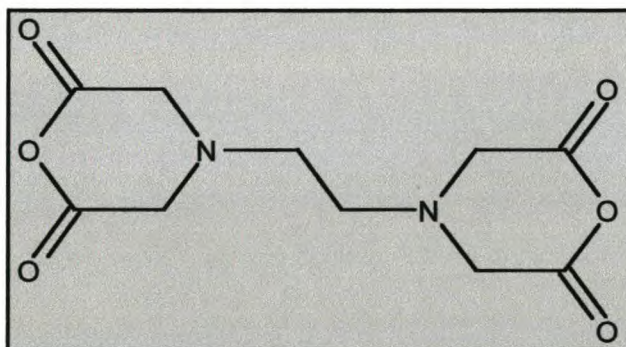


Table 4.1.1: Chemical shifts of ethylenediaminetetraacetic anhydride.

Dianhydride	^1H	^{13}C
$\text{NCH}_2\text{CH}_2\text{N}$	2.68	51.73
$-\text{CH}_2\text{COO}-$	3.72	52.20
$-\text{CH}_2\text{COO}-$		165.74

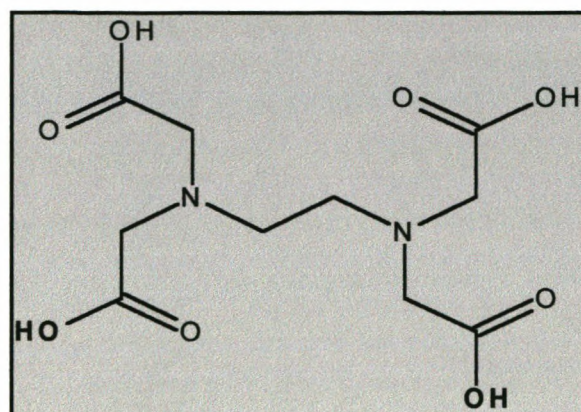
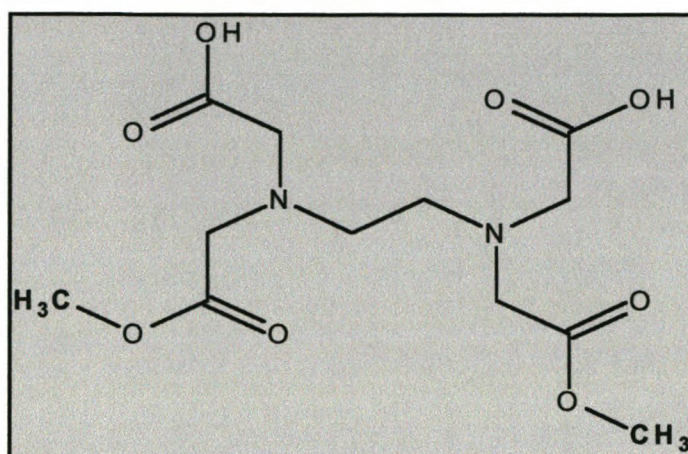


Table 4.1.2: Chemical shifts of ethylenediaminetetraacetic acid.

EDTA	¹ H	¹³ C
NCH ₂ CH ₂ N	2.78	51.55
-CH ₂ COOH	3.47	54.80
-CH ₂ COOH		172.45

Table 4.1.3: Chemical shifts of dimethyl *N,N'*-dicarboxymethyl-3,6-diazaoctanedioate.

DMDDO	^1H	^{13}C
$\text{NCH}_2\text{CH}_2\text{N}$	2.73	51.16
$-\text{CH}_2\text{COOH}$	3.43	54.35
$-\text{CH}_2\text{COOCH}_3$	3.55	54.09
$-\text{CH}_2\text{COOCH}_3$	3.60	50.89
$-\text{CH}_2\text{COOH}$		172.21
$-\text{CH}_2\text{COOCH}_3$		171.20

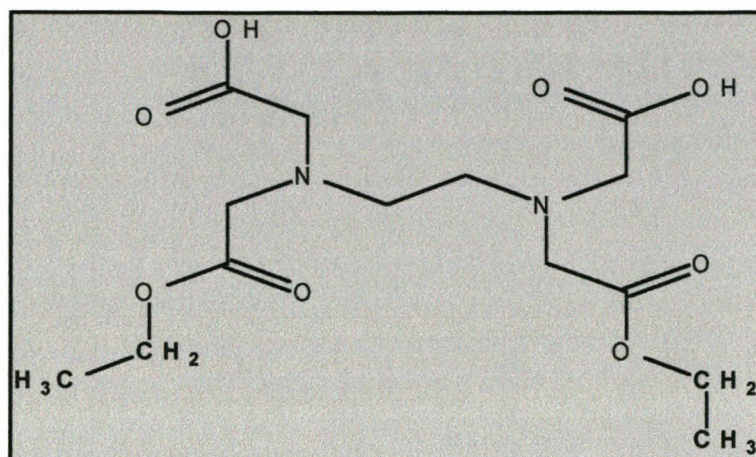


Table 4.1.4: Chemical shifts of diethyl *N,N'*-dicarboxymethyl-3,6-diazaoctanedioate.

DEDDO	^1H	^{13}C
$\text{NCH}_2\text{CH}_2\text{N}$	2.76	51.37
$-\text{CH}_2\text{COOH}$	3.46	54.53*
$-\text{CH}_2\text{COOCH}_2\text{CH}_3$	3.55	54.53*
$-\text{CH}_2\text{COOCH}_2\text{CH}_3$	4.09	59.78
$-\text{CH}_2\text{COOCH}_2\text{CH}_3$	1.19	13.92
$-\text{CH}_2\text{COOH}$		172.75
$-\text{CH}_2\text{COOCH}_2\text{CH}_3$		171.26

* These two peaks are exactly coincident

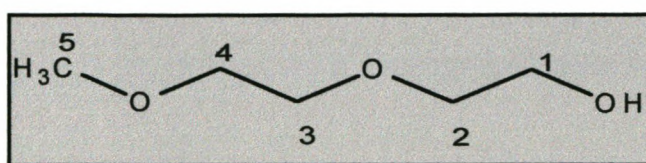


Table 4.1.5: Chemical shifts of diethyleneglycol monomethyl ether (DEGM).

DEGM	^1H	^{13}C
5	3.26	58.15
-OH	4.57 (Triplet)	
1 – 4	3.40 – 3.54 (Multiplet)	
1		60.37
2		72.51
3		69.73
4		71.49

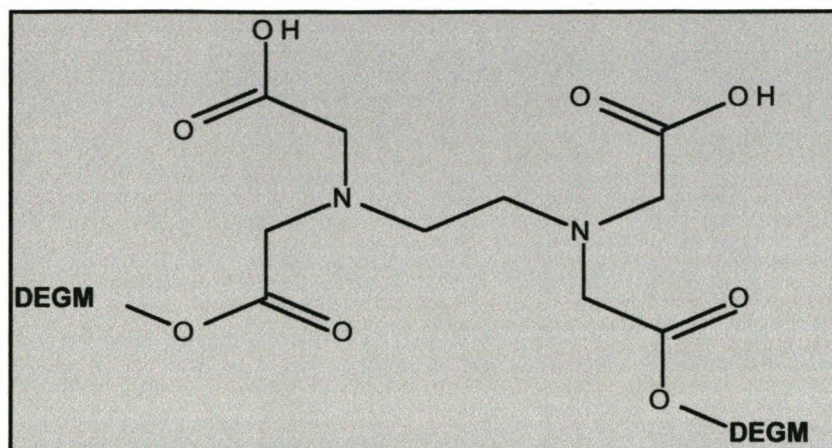


Table 4.1.6: Chemical shifts of bis[2(2-methoxyethoxy)ethyl] *N,N'*-dicarboxymethyl-3,6-diazaoctanedioate.

BMDDO	¹ H	¹³ C
NCH ₂ CH ₂ N	2.77	51.51
-CH ₂ COOH	3.46	54.67
-CH ₂ COODEGM	3.59	54.57
-CH ₂ COOH		172.94
-CH ₂ COODEGM		171.44
2-4	3.43 – 3.63 (Multiplet)	
1	4.17	63.27 (α)*
2		68.44 (β)*
3		69.77
4		71.45
5	3.26	58.21

* $\Delta\delta(\beta - \alpha) = 5,17$ ppm

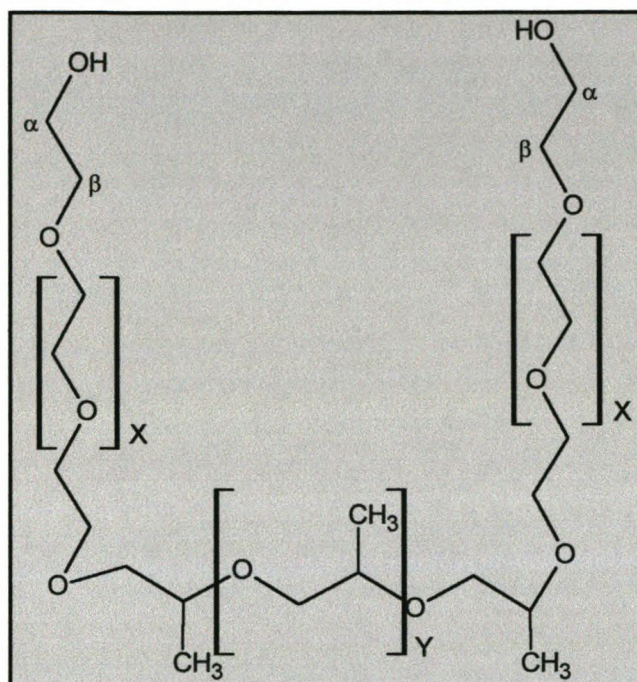


Table 4.1.7: Chemical shifts of Pluronic®F108.

Pluronic	^1H	^{13}C
$-\text{CH}_2-\text{CH}_2-\text{OH}$	3.75 – 3.78	60.40 (α)
$-\text{CH}_2-\text{CH}_2-\text{OH}$	3.62	73,09 (β)
$(\text{CH}_2-\text{CH}_2-\text{O})$	3.50 – 3.60 (3.53)	69.67 – 70.34 (70.00) [#]
$-\text{O}-\text{CHH}-\text{CH}(\text{CH}_3)-\text{O}$	3.28 – 3.36	72.50 – 72.70 (72.70) [#]
$-\text{O}-\text{CHH}-\text{CH}(\text{CH}_3)-\text{O}$	3.43 – 3.49	74.47 – 74.89 (74.80) [#]
$-\text{O}-\text{CHH}-\text{CH}(\text{CH}_3)-\text{O}$	1.03 and 1.05	17.17 – 17.27 (17.22) [#]

[#] = Highest peak

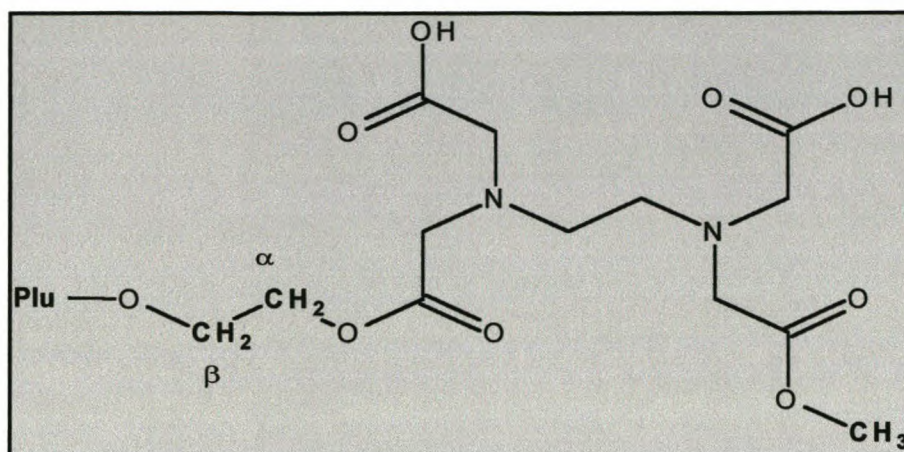


Table 4.1.8: Chemical shifts of the ligand-modified-Pluronic® F108.

Pluronic-DMDDO	^1H	^{13}C
$\text{NCH}_2\text{CH}_2\text{N}$	2.74 (Singlet with a	51.25
$\text{NCH}_2\text{CH}_2\text{N}$	shoulder)	51.07
$-\text{CH}_2\text{COOH}$	Coincident	54.36
$-\text{CH}_2\text{COO-Plu}$	3.56 (In footprint)	54.28
$-\text{CH}_2\text{COOCH}_3$	3.55 (In footprint)	54.17
$-\text{CH}_2\text{COOCH}_3$	3.61	50.96
$-\text{CH}_2\text{COOCH}_2\text{CH}_2\text{O-Plu}$	3.62 (Triplet)	62.96 (α)*
$-\text{CH}_2\text{COOCH}_2\text{CH}_2\text{O-Plu}$	Coincident	68.11 (β)*
$-\text{CH}_2\text{COOH}$		172.78
$-\text{CH}_2\text{COO-Plu}$		171.80
$-\text{CH}_2\text{COOCH}_3$		171.76
$(\text{CH}_2-\text{CH}_2-\text{O})$	3.47 – 3.51 (3.51)	69.66
$-\text{O-CHH-CH}(\text{CH}_3)-\text{O}$	3.22 – 3.33	72.13 – 72.33 (72.33) [#]
$-\text{O-CHH-CH}(\text{CH}_3)-\text{O}$	3.43 – 3.44	74.14 – 74.54 (74.46) [#]
$-\text{O-CHH-CH}(\text{CH}_3)-\text{O}$	1.03 and 1.04	17.06 – 17.17 (17.12) [#]

* $\Delta\delta (\beta - \alpha) = 5.15$ ppm[#] = Highest peak

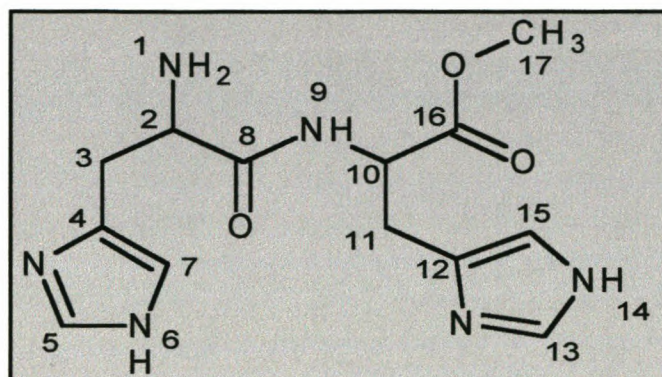


Table 4.1.9: Chemical shifts of L-histidyl-L-histidine methyl ester.[77]

His2	^1H	^{13}C
2	4.56 – 4.59 (Multiplet)	52.10
3	3.03 – 3.07 (Multiplet)	26.41
4		130.06
5	8.15	134.08
7	7.14	116.08
8		167.89
9	9.23 (Doublet)	
10	4.15 (Triplet)	52.19
11	3.12 – 3.17 (Multiplet)	27.62
12		130.46
13	8.51	134.69
15	7.28	118.07
16		170.40
17	3.64	51.68

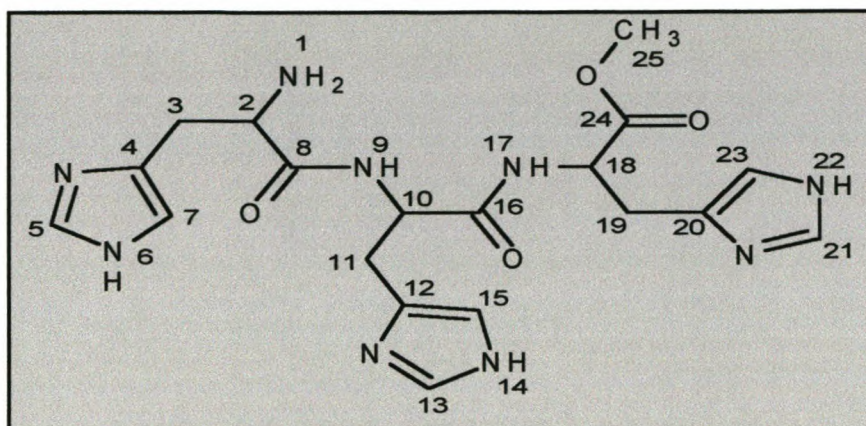


Table 4.1.10: Chemical shifts of L-histidyl-L-histidyl-L-histidine methyl ester.

His3	^1H	^{13}H
2	4.53 – 4.57 (Multiplet)	52.50
3, 11 & 19	2.97 – 3.13 (Multiplet)	
3		27.49
4		131.20
5	8.16	134.32
7	7.05	118.05
8		167.94
9	9.09 (Doublet)	
10	3.87 (Triplet)	52.22
11		27.92
12		131.68
13	7.75	135.07
15	6.98	115.61
16		170.13
17	8.95 (Doublet)	
18	4.05 (Triplet)	52.17
19		28.32
20		132.32
21	8.04	134.69
23	7.01	115.53
24		171.18
25	3.61	52.17

4.2. X-Ray diffraction data and crystal structures.

The crystal structures of CuDMDDO (see Fig.4.2.2.1 and Tables 4.2.1.1 – 4.2.1.3) and NiDEDDO(Im)₂ (see Fig. 4.2.2.1 and Tables 4.2.2.1 – 4.2.2.3) serve as proof for the potential use of these types of ligands in IMAC applications. From the structures it can be seen that the coordination is such as to leave the required bindings sites (adjacent) available for interaction with the bio-macromolecules.

The heteroatom-metal ion bond lengths and angles are in good correlation with similar types of complexes.[77-83]

4.2.1. CuDMDDO

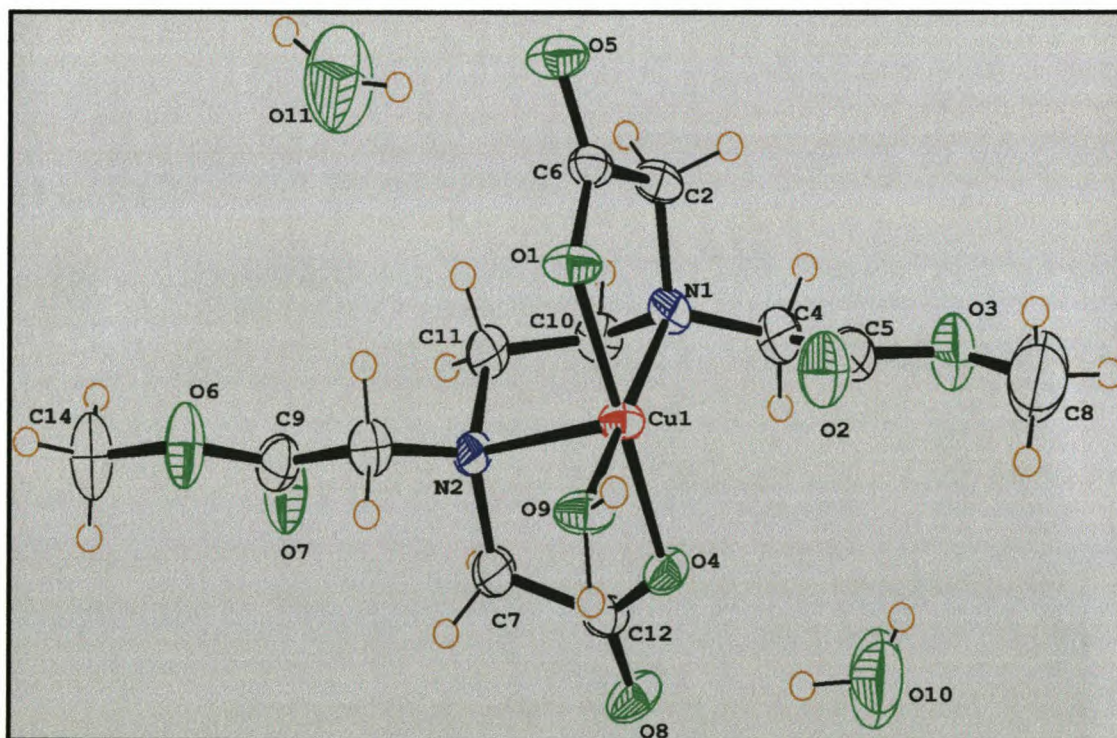


Figure 4.2.1.1: An Ortepe crystal structure of CuDMDDO - note the coordinated water molecule indicating the potential interaction site between the metal ion and protein. The thermal ellipsoids shown at the 50% probability level.

Table 4.2.1.1: Crystal data and structure refinement for CuDMDDO.

Empirical formula	C ₆ H ₁₁ Cu _{0.50} NO _{5.50}
Formula weight	216.93 g/mol
Temperature	173(2) K
Wavelength	0.71073 Å
Crystal system, space group	Monoclinic, P21
Unit cell dimensions	a = 7.5208(15) Å α = 90° b = 13.158(3) Å β = 104.31°(3) c = 9.5684(19) Å γ = 90°
Volume	917.5(3) Å ³
Z, Calculated density	4, 1.570 Mg/m ³
Absorption coefficient	1.249 mm ⁻¹
F(000)	450
Crystal size	0.37 x 0.25 x 0.12 mm
Theta range for data collection	2.20° to 27.54°
Limiting indices	-9 ≤ h ≤ 9, -17 ≤ k ≤ 15, -7 ≤ l ≤ 12
Completeness to theta = 27.54	98.2%
Absorption correction	None
Reflections collected / unique	5091 / 3673 [R(int) = 0.0248]
Refinement method	Full-matrix least-squares on F ²
Data / restraints / parameters	3673 / 7 / 256
Goodness-of-fit on F ²	1.030
Final R indices [I > 2σ(I)]	R1 = 0.0359, wR2 = 0.0737
R indices (all data)	R1 = 0.0457, wR2 = 0.0775
Absolute structure parameter	0.020(14)
Extinction coefficient	0.0033(14)
Largest diff. peak and hole	0.380 and -0.315 e.Å ⁻³

Table 4.2.1.2: The important bond lengths (Å) for CuDMDDO.

Bonds	Bond lengths (Å)
Cu(1)-O(1)	1.917(2)
Cu(1)-O(4)	1.951(2)
Cu(1)-O(9)	1.959(2)
Cu(1)-N(1)	2.080(3)
Cu(1)-N(2)	2.326(3)

Table 4.2.1.3: The important bond angles for CuDMDDO.

Bonds	Bond angles (°)
O(1)-Cu(1)-O(4)	176.62(11)
O(1)-Cu(1)-O(9)	88.26(10)
O(4)-Cu(1)-O(9)	94.48(10)
O(1)-Cu(1)-N(1)	85.28(9)
O(4)-Cu(1)-N(1)	92.22(10)
O(9)-Cu(1)-N(1)	170.73(12)
O(1)-Cu(1)-N(2)	96.74(10)
O(4)-Cu(1)-N(2)	80.73(9)
O(9)-Cu(1)-N(2)	103.05(10)
N(1)-Cu(1)-N(2)	84.33(10)

Symmetry transformations used to generate equivalent atoms:

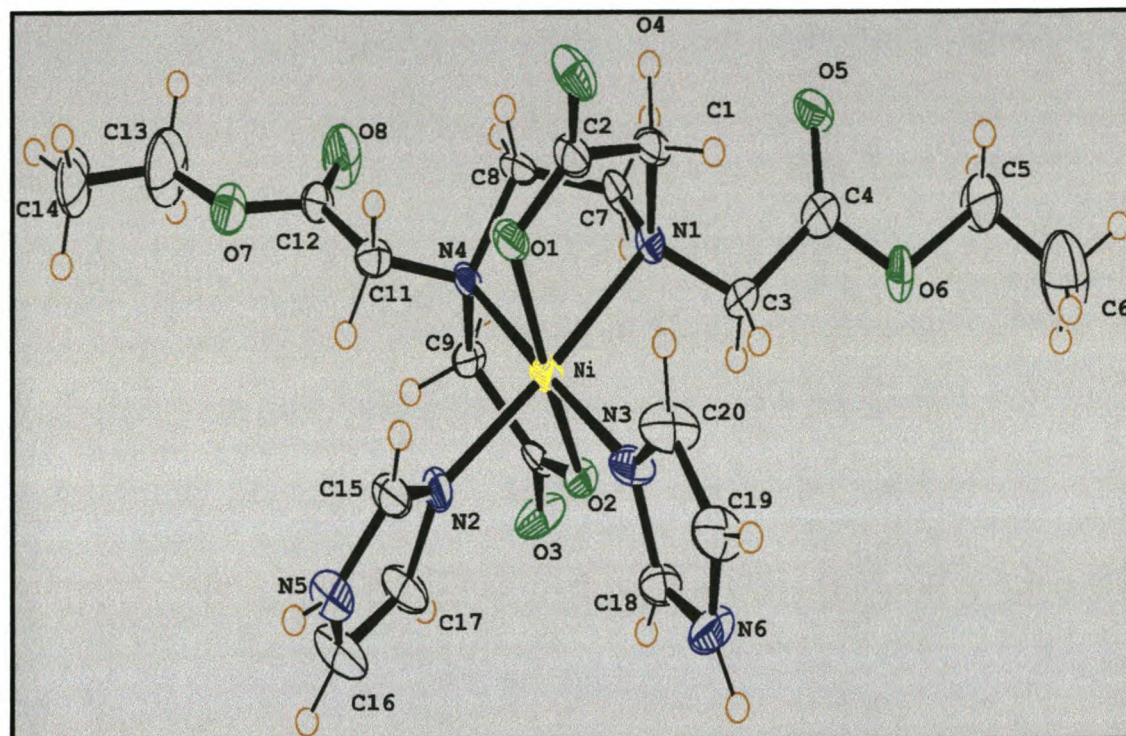
4.2.2. NiDMDDO(Im)₂

Figure 4.2.2.1: An Ortep crystal structure of NiDEDDO(Im)₂ - note the two imidazole groups indicating the potential interaction sites between the metal ion and the protein. The thermal ellipsoids shown at the 50% probability level.

Table 4.2.2.1: Crystal data and structure refinement for NiDMDDO(Im)₂.

Empirical formula	C ₂₀ H ₃₀ N ₆ NiO ₈
Formula weight	541.21 g/mol
Temperature	173(2) K
Wavelength	0.71073 Å
Crystal system, space group	Monoclinic, P21/n
Unit cell dimensions	a = 8.3664(17) Å α = 90° b = 25.367(5) Å β = 109.29°(3) c = 12.624(3) Å γ = 90°
Volume	2528.7(9) Å ³
Z, Calculated density	4, 1.422 Mg/m ³
Absorption coefficient	0.822 mm ⁻¹
F(000)	1136
Crystal size	0.25 x 0.07 x 0.05 mm
Theta range for data collection	1.61° to 25.72°
Limiting indices	-7 ≤ h ≤ 8, -30 ≤ k ≤ 30, -9 ≤ l ≤ 15
Reflections collected / unique	7625 / 4089 [R(int) = 0.0630]
Completeness to theta = 25.72	82.7%
Max. and min. transmission	0.9601 and 0.8209
Refinement method	Full-matrix least-squares on F ²
Data / restraints / parameters	4089 / 0 / 316
Goodness-of-fit on F ²	0.867
Final R indices [I > 2σ(I)]	R1 = 0.0740, wR2 = 0.1497
R indices (all data)	R1 = 0.1463, wR2 = 0.1778
Largest diff. peak and hole	0.730 and -0.368 e.Å ⁻³

Table 4.2.2.2: The important bond lengths (Å) for NiDMDDO(Im)₂.

Bonds	Bond length (Å)
Ni-O(1)	2.049(5)
Ni-O(2)	2.048(5)
Ni-N(3)	2.063(6)
Ni-N(2)	2.075(6)
Ni-N(1)	2.169(6)
Ni-N(4)	2.167(6)

Table 4.2.2.3: The important bond angles for NiDMDDO(Im)₂.

Bonds	Bond angles (°)
O(1)-Ni-O(2)	171.6(2)
O(1)-Ni-N(3)	91.1(2)
O(2)-Ni-N(3)	95.1(2)
O(1)-Ni-N(2)	94.2(2)
O(2)-Ni-N(2)	91.6(2)
N(3)-Ni-N(2)	88.8(2)
O(1)-Ni-N(1)	82.3(2)
O(2)-Ni-N(1)	91.6(2)
N(3)-Ni-N(1)	93.9(2)
N(2)-Ni-N(1)	175.7(2)
O(1)-Ni-N(4)	90.6(2)
O(2)-Ni-N(4)	83.0(2)
N(3)-Ni-N(4)	176.8(3)
N(2)-Ni-N(4)	93.9(2)
N(1)-Ni-N(4)	83.6(2)

Symmetry transformations used to generate equivalent atoms:

4.3. Infra Red spectroscopy results.

The infrared spectra of the ligands and the metal complexes (see Table 4.3.1) were obtained in crystalline state as KBr pellets. The metal complex spectra differ substantially from that of the free ligand, which is a positive indicator of coordination around the metal ion.

The most significant spectral feature for the complexes is the strong band around 1610 cm^{-1} , characteristic of the $\nu(\text{C}=\text{O})$ of a coordinated carboxyl group. Most of the complex spectra exhibit a broad band in the region of 3400 cm^{-1} , which indicate the possible presence of coordinated and/or lattice water.

Evidence for the carboxyl group coordinating to the metal ion is found in the shift and increase in intensity of the $\nu(\text{C}=\text{O})$, from around 1630 cm^{-1} for the free ligand to around 1610 cm^{-1} for the coordinated ligand. For example the band at 1632 cm^{-1} in DMDDO shifts to 1606 cm^{-1} in the nickel complex and to 1610 cm^{-1} in the copper complex.

This shift is not observed for the EDDA complexes because the ligand spectrum as reference exhibits strong hydrogen-bonded $-\text{COOH}$ groups with the $\nu(\text{C}=\text{O})$ band occurring at 1582 cm^{-1} with a shoulder at 1612 cm^{-1} .

The second largest shift occurs for the $\nu(\text{C}=\text{O})$ of the ester function of the ligand. The band at 1750 cm^{-1} of the free DMDDO is shifted by $13 - 11\text{ cm}^{-1}$ in the spectra of the nickel and copper complexes.[75;78-82]

The spectrum of CuDEDDO shows a split band for both the $\nu(\text{C}=\text{O})$ and $\nu(\text{C}-\text{O})$ of the ester group and could indicate a non-equivalence of both groups in the crystalline state.

Table 4.3.1: Infrared absorbencies with intensities and assignments for the ligands and complexes. See Table 4.3.2 explanation of abbreviations used.

EDDA ligand	NiEDDA	CuEDDA	Assignment
	3278 (vs)	3247 (s)	v(N-H)
	3253 (s)	3223-25 (s)	
1612 (sh)		1610 (vvs)	v(C=O)
1582 (vvs)	1583 (vvs)	1590 (vvs)	
1469 (sh)	1459 (m)	1469 (m)	δ (C-H) deformation
1452 (s)	1451 (m)	1454 (m)	
1430 (s)		1430-34 (m)	
1232 (ms)	1226 (w)	1235 (mw)	v(C-O)

DMDDO ligand	NiDMDDO	CuDMDDO	Assignment
3474 (w)		3443 (s,br)	v(O-H)
	~3400 (s,br)		Co-ordinated water
3024 (m)			
2996 (w)			v(C-H)
2967 (m)	2954 (m)	2956 (m)	
1750 (vvs)	1737-9 (vs)	1739 (vs)	v(C=O) ester
1632 (s)	1606-8 (vvs)	1610 (vvs)	v(C=O) carboxyl
1471 (sh)			
1444 (s)	1438-9 (s)	1436 (m)	δ (CH) deformation
1402 (s)	1398-9 (vs)	1381-2 (s)	
1241 (vs)		1255 (sh)	v(C-O) carboxyl
1216 (s)	1211-2 (vs)	1221-2 (s)	
1087 (m)	1112 (s)	1117-8 (s)	v(C-O) ester

	NiDEDDO	CuDEDDO	Assignment
3457 (w)			v(O-H)
	3391 (s,br)		Co-ordinated water
3007 (sh)			
2986 (m)	2982 (m)	2980 (m)	
2940 (m)	2943 (m)	2937 (m)	v(C-H)
2916 (w,br)			
1742 (vvs)	1735 (vs)	1736 (vs)	
1713 (s,sh)		1728 (vs)	v(C=O) ester
1638 (m)	1610 (vvs)	1611 (vvs)	v(C=O) carboxyl
1477 (s)			
1455 (m)		1452 (m)	
1444 (w)		1434 (m)	
1422 (s)		1416 (m)	δ (CH) deformation
1403 (m)			
1387 (m)	1395 (vs)	1381 (vs)	
1205 (vs)	1204 (s)	1214 (vs)	v(C-O) carboxyl
1112 (m)	1110 (m)	1114 (s)	v(C-O) ester
		1100 (sh)	
694 (s)		708 (w)	CH ₂ rocking

NiDMDDO(lm)₂	Assignment
3456 (m,br)	$\nu(\text{O-H})$
3168 (m)	
3155 (m)	$\nu(\text{C-H})$ imidazole
3092 (m)	
3016 (m)	
2972 (w)	$\nu(\text{C-H})$
2944 (s)	
1736 (vs)	$\nu(\text{C=O})$ ester
1616 (vvs)	$\nu(\text{C=O})$ carboxyl
1596 (vvs)	
1541 (m)	$\nu(\text{C-C}) + \nu(\text{C-N})$
1494 (w)	imidazole
1451 (m)	$\delta(\text{CH})$ deformation
1435 (ms)	
1422 (m)	$\nu(\text{C-C}) + \nu(\text{C-N})$ imidazole
1398 (s)	$\delta(\text{CH})$ deformation
1329-24 (w)	$\nu(\text{C-C}) + \nu(\text{C-H})$ imidazole
1263 (sh)	
1205 (s)	$\nu(\text{C-O})$ carboxyl
1151 (w)	$\nu(\text{C-C}) + \nu(\text{C-N})$ imidazole
1112 (s)	$\nu(\text{C-O})$ ester
1094 (m)	$\nu(\text{C-C}) + \nu(\text{C-N})$ imidazole
1079 (s)	$\nu(\text{C-N}) + \delta(\text{C-H})$ imidazole
846 (mw)	$\gamma(\text{C-H})$ imidazole

NiDEDDO(Im)₂	Assignment
3148 (m)	
3106 (m)	v(C-H) imidazole
3020 (m)	
2937 (s)	v(C-H)
1748 (vs)	v(C=O) ester
1590 (vvs)	v(C=O) carboxyl
1548 (sh)	v(C-C) + v(C-N)
1507 (w)	imidazole
1477 (w)	
1455 (m)	δ (CH) deformation
1444 (m)	
1421 (m)	v(C-C) + v(C-N) imidazole
1332 (m)	v(C-N) + δ (C-H) imidazole
1248 (w)	v(C-N) + δ (C-H) imidazole
1222 (sh)	v(C-O) carboxyl
1194 (vs)	
1095 (s)	v(C-C) + n(C-N) imidazole
1072-67 (s)	v(C-N) + δ (C-H) imidazole
1030 (m)	v(C-O) ester
922 (m)	Imidazole
842-34 (m)	γ (C-H)
812 (w)	γ (C-H) imidazole
750 (w)	CH ₂ rocking
660 (ms)	Imidazole

Table 4.3.2: Explanation of the abbreviations used in Table 4.3.1

m	medium
m,br	medium and broad
ms	medium strong
mw	medium weak
s	strong
s,sh	strong with shoulder
sh	shoulder
vs	very strong
vvs	very very strong
w	weak
w,br	weak and broad
ν	stretching vibration
δ	deformation vibration
γ	rocking vibration

4.4. Mass spectrometry

4.4.1. Electron Impact Mass spectrometry (EI-MS)

Ligand	MW	Largest ion	Assignment	Evap. Temp
EDDA	176,17	158	$[M-H_2O]^+$	220°C
DMDDO	320,30	320	$[M]^+$	135°C
DEDDO	348,36	348	$[M]^+$	130°C

Ni complex	MW	Observed MS peak
NiEDDA	232,35	233
NiDMDDO	376,98	377
NiDMDDO(Im) ₂	513,14	377 (512)
NiDEDDO	405,03	405
NiDEDDO(Im) ₂	541,19	405 (540)

Cu complex	MW	Observed MS peak
CuEDDA	237,70	238 (weak response)
CuDMDDO	381,83	382
CuDEDDO	409,89	410

4.4.2. Electrospray Ionisation Mass spectrometry.[84]**4.4.2.1. Nickel complexes:****NiEDDA (232,35 g/mol)**

Method: ES-positive ions.

Solvent: Methanol/water.

Molecular ion peak: $233 = [^{58}\text{Ni-Ligand} + \text{H}]^+$ and $255 = [232 + \text{Na}]^+$

Dimer: $465 = [2 \times 232 + \text{H}]^+$ and $487 = [2 \times 232 + \text{Na}]^+$

Trimer: $697 = [3 \times 232 + \text{H}]^+$ and $719 = [3 \times 232 + \text{Na}]^+$

Tetramer: $929 = [4 \times 232 + \text{H}]^+$ and $951 = [4 \times 232 + \text{Na}]^+$

MW: 232 g/mol based on ^{58}Ni

Formula: $\text{C}_6\text{H}_{10}\text{N}_2\text{NiO}_4$

NiDMDDO (376,98 g/mol)

Method: ES-positive ions.

Solvent: Methanol/water.

Molecular ion peak: $377 = [^{58}\text{Ni-Ligand} + \text{H}]^+$ and $399 = [376 + \text{Na}]^+$

Dimer: $753 = [2 \times 376 + \text{H}]^+$ and $775 = [2 \times 376 + \text{Na}]^+$

MW: 376 g/mol based on ^{58}Ni

Formula: $\text{C}_{12}\text{H}_{18}\text{N}_2\text{NiO}_8$

NiDMDDO(Im)₂ (513,14 g/mol)

Method: ES-positive ions.

Solvent: Methanol/water.

Molecular ion peak: $377 = [^{58}\text{Ni-Ligand} + \text{H}]^+$ and $399 = [376 + \text{Na}]^+$

Dimer: $753 = [2 \times 376 + \text{H}]^+$ and $775 = [2 \times 376 + \text{Na}]^+$

MW: 376 g/mol based on ^{58}Ni (without 2 x Im-68) otherwise would 512 be possible.

Formula: $\text{C}_{12}\text{H}_{18}\text{N}_2\text{NiO}_8$

Remarks: This spectrum is identical to that of NiDMDDO. It seems the imidazole does not co-ordinate very strongly and that it is removed from the rest of the complex during the ionisation process.

NiDEDDO (405,03 g/mol)

Method: ES-positive ions.

Solvent: Methanol/water.

Molecular ion peak: $405 = [^{58}\text{Ni-Ligand} + \text{H}]^+$ and $427 = [404 + \text{Na}]^+$

Dimer: $809 = [2 \times 404 + \text{H}]^+$ and $831 = [2 \times 404 + \text{Na}]^+$

MW: 404 g/mol based on ^{58}Ni

Formula: $\text{C}_{14}\text{H}_{22}\text{N}_2\text{NiO}_8$

NiDEDDO(Im)₂ (541,19 g/mol)

Method: ES-positive ions.

Solvent: Methanol/water.

Molecular ion peak: $405 = [^{58}\text{Ni-Ligand} + \text{H}]^+$ and $427 = [404 + \text{Na}]^+$

Dimer: $809 = [2 \times 404 + \text{H}]^+$ and $831 = [2 \times 404 + \text{Na}]^+$

MW: 404 g/mol based on ^{58}Ni (without 2x Im-68) otherwise 540 would be possible.

Formula: $\text{C}_{14}\text{H}_{22}\text{N}_2\text{NiO}_8$

Remarks: This spectrum is almost identical to that of NiDEDDO. Again it seems that the imidazole does not co-ordinate very strongly and is lost from the complex during ionisation.

4.4.2.2. Copper complexes**CuEDDA (237,70 g/mol)**

Method: ES-positive ions.

Solvent: Methanol/water.

Molecular ion peak: $238 = [{}^{63}\text{Cu-Ligand} + \text{H}]^+$

Dimer: $475 = [2 \times 237 + \text{H}]^+$ and $497 = [2 \times 237 + \text{Na}]^+$

Trimer: $712 = [3 \times 237 + \text{H}]^+$ and $734 = [3 \times 237 + \text{Na}]^+$

MW: 237 g/mol based on ${}^{63}\text{Cu}$

Formula: $\text{C}_6\text{H}_{10}\text{CuN}_2\text{O}_4$

Remarks: Weak spectrum due to weak responses.

CuDMDDO (381,83 g/mol)

Method: ES-positive ions.

Solvent: Methanol/water.

Molecular ion peak: $382 = [{}^{63}\text{Cu-Ligand} + \text{H}]^+$ and $404 = [381 + \text{Na}]^+$

Dimer: $763 = [2 \times 381 + \text{H}]^+$ and $785 = [2 \times 381 + \text{Na}]^+$

MW: 381 g/mol based on ${}^{63}\text{Cu}$

Formula: $\text{C}_{12}\text{H}_{18}\text{CuN}_2\text{O}_8$

Remarks: Decarboxylation ($-\text{CO}_2 = 44$) assigned to 338 and 719.

CuDEDDO (409,89 g/mol)

Method: ES-positive ions.

Solvent: Methanol/water.

Molecular ion peak: $410 = [{}^{63}\text{Cu-Ligand} + \text{H}]^+$ and $432 = [409 + \text{Na}]^+$

Dimer: $819 = [2 \times 409 + \text{H}]^+$ and $841 = [2 \times 409 + \text{Na}]^+$

MW: 409 g/mol based on ${}^{63}\text{Cu}$

Formula: $\text{C}_{14}\text{H}_{22}\text{CuN}_2\text{O}_8$

Remarks: Decarboxylation ($-\text{CO}_2 = 44$) assigned to 366 and 775.

L-Histidyl-L-histidine methyl ester (His2).

Method: ES-positive ions, cone voltage = 15 V.

Solvent: 50% acetonitrile, 0,1% formic acid

Molecular ion peak: 307 = [His2 + H]⁺ and 154 = [His2 + 2H]²⁺

MW: 306 g/mol

Formula: C₁₃H₁₈N₆O₃

L-Histidyl-L-histidyl-L-histidine methyl ester (His3)

Method: ES-positive ions, cone voltage = 20 V.

Solvent: 50% acetonitrile, 0,1% formic acid

Molecular ion peak: 444 = [His3 + H]⁺ and 222 = [His3 + 2H]²⁺

MW: 443 g/mol

Formula: C₁₉H₂₅N₉O₄

4.5. UV-VIS spectroscopy

UV-VIS spectroscopy was used to qualitatively determine if the ligand modified Pluronic did indeed chelate metal ions. It should be remembered that Pluronic is a bulky molecule (14600 Da), thus as was the case with NMR, the changes are very subtle and that the PEO-PPO-PEO backbone have a major influence on the spectra, drowning to an extent the absorbance of the ligand end-groups.

From Fig. 4.5.1 can be seen, that the spectra of the ligand modified Pluronic differs considerably from that of unmodified Pluronic and that there are some similarities (190 – 200 nm) to the model ligand DMDDO.

In fig. 4.5.3 (UV) and fig.4.5.5 (VIS) similarities are observed between the copper chelated ligand-modified-Pluronic and the model complex CuDMDDO. Ligand modified Pluronic and unmodified Pluronic have hardly any absorbance in the visible part of the spectrum.

Absorptivity values (see Table 4.5.1) indicate a considerable difference between ligand modified- and unmodified Pluronic as well as an increase in absorptivity when Cu^{2+} ions are added to the ligand modified Pluronic. The absorptivity values for the ligand-modified-Pluronic is more than twice as much for unmodified Pluronic at 193 nm. When the Cu^{2+} was chelated with DMDDO the absorptivity value increased more than three times. A similar increase was observed for the Cu^{2+} -ligand-modified-Pluronic solution. This sharp increase is a definite indication that metal chelation is taking place. There was also a slight increase in absorption in the visible region taken at 738 nm.

The very slight increase in absorptivity of unmodified Pluronic after reaction with the copper might be because of the PEO blocks acting as crown-ethers, wrapping themselves around the copper ions allowing for an increase in absorbance.

Table 4.5.1: Table correlating the absorptivity ($\text{cm}^{-1}\text{g}^{-1}\text{L}$) of the different solutions to their concentration. Absorptivity values were calculated for absorbencies in the UV-region at 193 nm and for the VIS-region of the spectrum at 738 nm.

	Conc. (M)	Conc. (g/L)	Absorbance ($A_{193 \text{ nm}}$)	Absorptivity ($a_{193 \text{ nm}}$)
DMDDO	$2,0 \cdot 10^{-4}$	0,08	0,4933	6,46
Modified Pluronic		0,60	0,4772	0,80
Pluronic		1,00	0,3579	0,36
CuDMDDO	$1,0 \cdot 10^{-4}$	0,04	0,7863	20,59
Cu + Modified Pluronic		0,25	1,0371	4,15
Cu + Pluronic		1,00	0,5867	0,59
			($A_{738 \text{ nm}}$)	($a_{738 \text{ nm}}$)
CuDMDDO	$2,0 \cdot 10^{-3}$	0,76	0,1056	0,14
Cu + Modified Pluronic		5,00	0,0574	0,01
Cu + Pluronic		1,00	0,0028	0,00
DMDDO	$2,0 \cdot 10^{-4}$	0,08	0,0017	0,02
Modified Pluronic		0,60	0,0010	0,00
Pluronic		1,00	0,0007	0,00

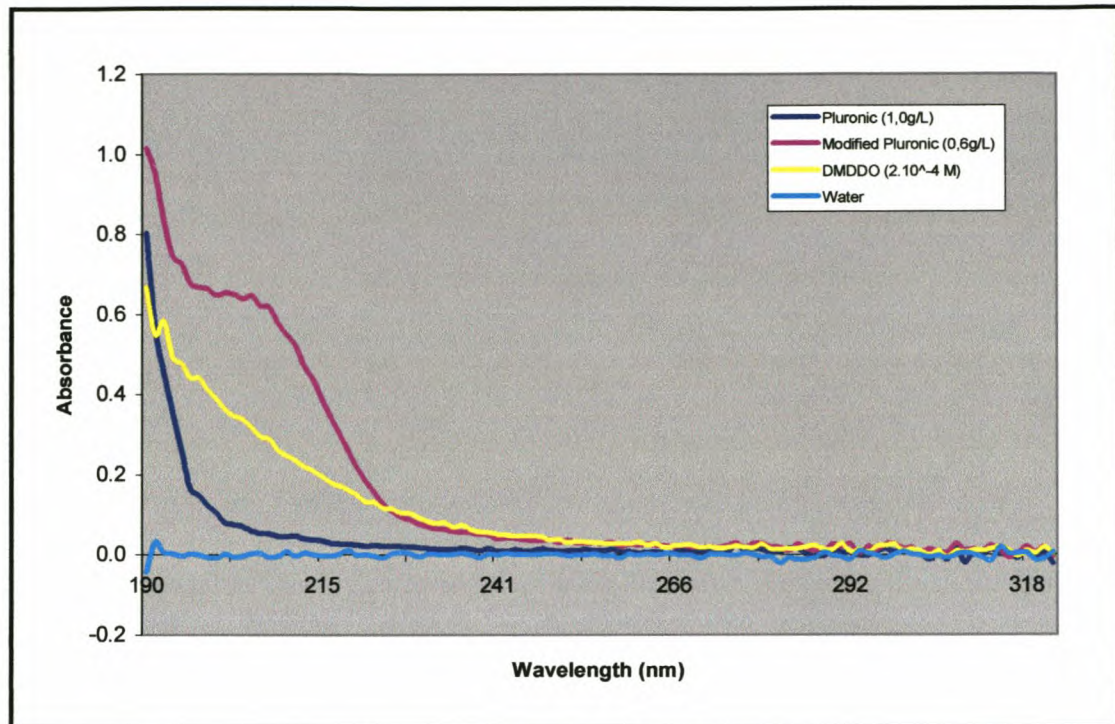


Figure 4.5.1: UV-spectra comparison between Pluronic, ligand-modified-Pluronic and the model ligand DMDDO.

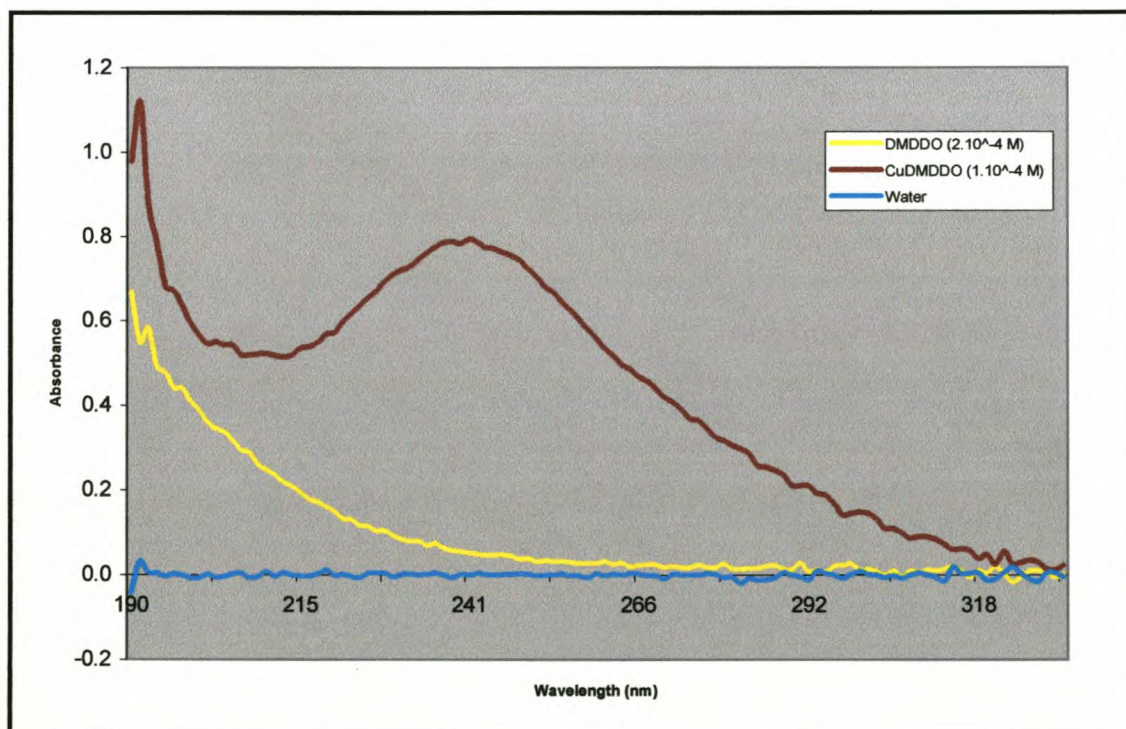


Figure 4.5.2: UV-spectra comparison between the model ligand DMDDO and its model copper complex CuDMDDO.

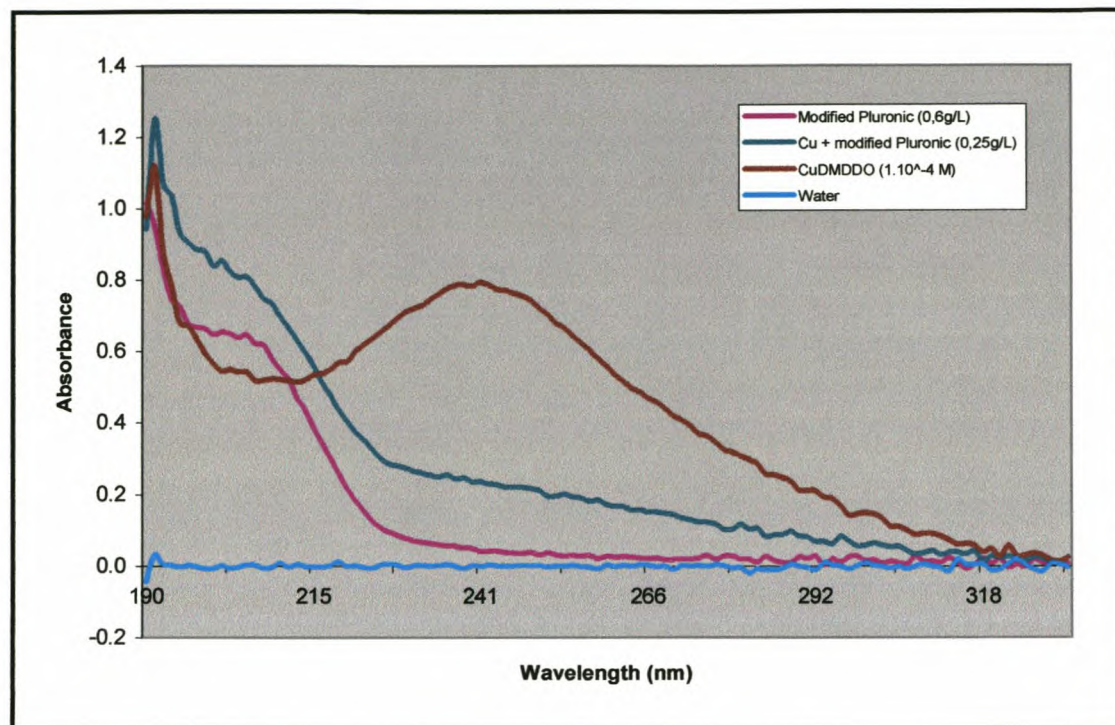


Figure 4.5.3: UV-spectra comparison between modified Pluronic, Cu²⁺ + ligand-modified-Pluronic and CuDMDDO.

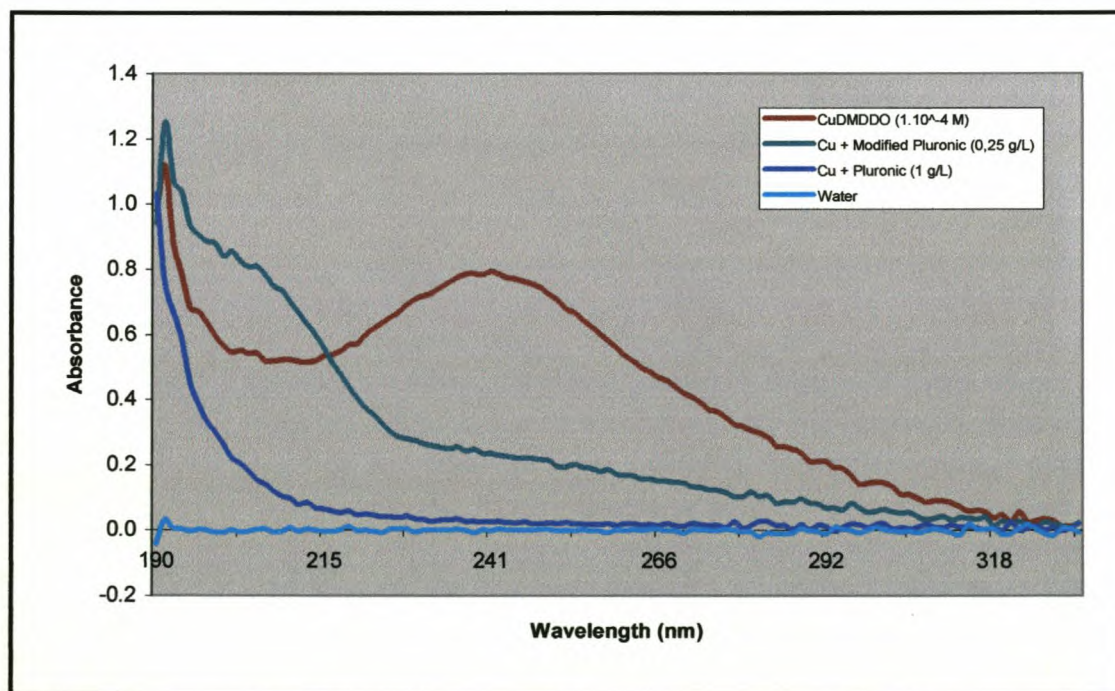


Figure 4.5.4: UV-spectra comparison between CuDMDDO, Cu²⁺ + ligand modified Pluronic and Cu²⁺ + Pluronic.

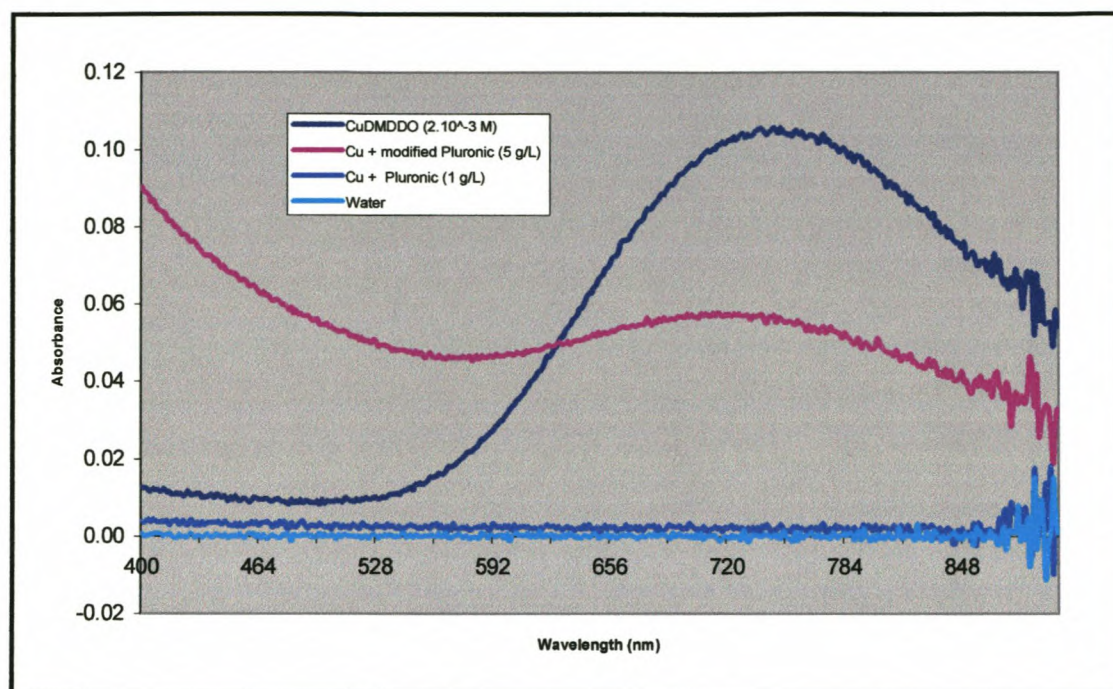


Figure 4.5.5: VIS-spectra comparison between CuDMDDO and Cu²⁺ + ligand-modified-Pluronic.

Chapter 5: Conclusion.

In these first steps towards putting into place an immobilized metal affinity system for application in large-scale operations, model ligands (DEDDO and DMDDO) and their nickel and copper complexes were synthesised and characterised. X-ray crystal structures of CuDMDDO and NiDEDDO(Im)₂ have shown the required vacant coordination sites on the metal ions for interaction with bio-macromolecules.

The model peptides His2 and His3 were also synthesised for the use in coordination studies to model the poly-histidine affinity tag's interaction with metal ions chelated by the ligand type used in this study. These peptides will also be used in initial studies to test the separation effectiveness of the assembled metal affinity separation system.

A synthesis procedure was developed, through model reactions (MMDDO), to couple Pluronic[®] F108, which acts as the support matrix, to the ligand. The ligand-modified-Pluronic was characterised by means of NMR by comparing the spectra of the model ligands to that of the ligand-modified-Pluronic.

The ligand-modified-Pluronic was tested, qualitatively in solution, for its metal chelating abilities. This was done by means of UV-VIS spectroscopy. From the spectra substantial differences were observed between unmodified- and modified Pluronic. The spectra of these compounds after reacting them with Cu²⁺, indicated that metal chelation is taking place by the ligand-modified-Pluronic.

Chapter 6: Future work.

Ligands: Future work entails determining pKa values for the model ligand. This can be done by potentiometric titrations.

Simpler, but similar ligands can be investigated to reduce possible steric hindrance. One of the methyl carboxymethyl groups in the DMDDO ligand is not taking part in metal chelation or attachment to the support matrix and might interfere with the protein's interaction with the immobilised metal ion. This methyl carboxymethyl group can be made redundant. Figure 6.1. shows two possible alternative ligands.

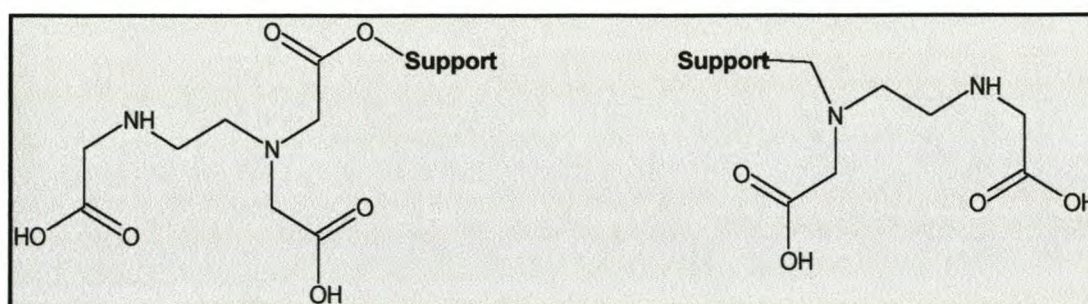


Figure 6.1: Two alternative ligands to DMDDO.

Model complexes: Further work can be carried out on the model complexes, this includes the determination of stability constants of the current complexes, replacing imidazole with His2 and His3 in the reaction mixtures and investigating these complexes by UV-VIS spectroscopy. There are definite colour changes when these di- and tri-peptides are introduced which suggest coordination. ES-MS might also give valuable insight into the coordination of His2 and His3 with the model complexes NiDMDDO and CuDMDDO.

Modified Pluronic: The percentage conversion of Pluronic to ligand modified Pluronic still needs to be determined. This can be determined by titrating the acid groups of the ligand with a base.

The adsorption and desorption characteristics of modified Pluronic onto the membrane surface and subsequent quantitative determination of metal ion chelation

abilities will also needed to be investigated. Quantitative studies, of the metal ion binding capabilities, can be performed by mass balance experiments with the aid of atomic absorption- (AA) or inductive coupled plasma mass spectroscopy (ICP-MS).

Initial experiments for protein retention effectiveness can be investigated by studying the retention of His2 and His3 by the system before moving onto more complex protein retention experiments.

References

1. Porath, J.; Carlsson, J.; Olsson, I.; Belfrage, G. *Nature* **1975**, *258*, 598-599.
2. Hochuli, E.; Döbeli, H.; Schacher, A. *Journal of Chromatography* **1987**, *411*, 177-184.
3. Wong, J.W.; Albright, R.L.; Wang, N.L. *Separation and Purification Methods* **1991**, *20*, 49-106.
4. Sidenius, U.; Farver, O.; Jøns, O.; Gammelgaard, B. *Journal of Chromatography B* **1999**, *735*, 85-91.
5. Fitton, V.; Santarelli, X. *Journal of Chromatography B* **2001**, *754*, 135-140.
6. Chaouk, H.; Hearn, M.T.W. *Journal of Chromatography A* **1999**, *852*, 105-115.
7. Boden, V.; Winzerling, J.J.; Vijayalakshmi, M.A.; Porath, J. *Journal of Immunological Methods* **1995**, *181*, 225-232.
8. Berna, P.P.; Mrabet, N.T.; Van Beeumen, J.; Devreese, B.; Porath, J.; Vijayalakshmi, M.A. *Biochemistry* **1997**, *36*, 6896-6905.
9. Abubiab, T.; Beitle, R.R. *Journal of Chromatography A* **1998**, *795*, 211-217.
10. Liesiene, J.; Raceityte, K.; Morkeviciene, M.; Valancius, P.; Brumelis, V. *Journal of Chromatography A* **1997**, *764*, 27-33.
11. Zeng, Q.; Xu, J.; Ru, R.; Ye, Q. *Journal of Chromatography A* **2001**, *921*, 197-205.
12. Porath, J. *Journal of Chromatography* **1988**, *443*, 3-11.
13. Yip, T.; Nakagawa, Y.; Porath, J. *Analytical Biochemistry* **1989**, *183*, 159-171.
14. Belew, M.; Yip, T.-T.; Andersson, L.; Porath, J. *Journal of Chromatography* **1987**, *403*, 197-206.
15. Haupt, K.; Roy, F.; Vijayalakshmi, M.A. *Analytical Biochemistry* **1996**, *234*, 149-154.
16. El Rassi, Z.; Truel, Y.; Maa, Y.-F.; Horváth, C. *Analytical Biochemistry* **1988**, *169*, 172-180.
17. El Rassi, Z.; Horváth, C. *Journal of Chromatography* **1986**, *359*, 241-253.
18. Porath, J.; Olin, B. *Biochemistry* **1983**, *22*, 1621-1630.
19. Hemdan, E.S.; Porath, J. *Journal of Chromatography* **1985**, *323*, 247-254.

References

20. Ramadan, N.; Porath, J. *Journal of Chromatography* **1985**, *321*, 81-91.
21. Hochuli, E.; Bannwarth, W.; Döbeli, H.; Gentz, R.; über, D. *Biotechnology* **1988**, *Nov*, 1321-1325.
22. Kronina, V.V.; Wirth, H.-J.; Hearn, M.T.W. *Journal of Chromatography A* **1999**, *852*, 261-272.
23. Arvidsson, P.; Ivanov, A.E.; Galaev, I.Y.; Mattiasson, B. *Journal of Chromatography B* **2001**, *753*, 279-285.
24. Enzelberger, M.M.; Minning, S.; Schmid, R.D. *Journal of Chromatography A* **2000**, *898*, 83-94.
25. Clemmit, R.H.; Chase, H.A. *Journal of Chromatography A* **2000**, *874*, 27-43.
26. Gibert, S.; Bakalara, N.; Santarelli, X. *Journal of Chromatography B* **2000**, *737*, 143-150.
27. Johnson, R.D.; Arnold, F.H. *Biotechnology and Bioengineering* **1995**, *48*, 437-443.
28. Sulkowski, E. *BioEssays* **1989**, *10*, 170-175.
29. Hochuli, E. *Journal of Chromatography A* **1988**, *444*, 293-302.
30. Beitle, R.R.; Atai, M.M. *AIChE Symposium Series* **199**, *88*, 34-44.
31. Arnold, F.H. *Biotechnology* **1991**, *9*, 151-156.
32. Ramadan, N.; Porath, J. *Journal of Chromatography* **1985**, *321*, 93-113.
33. Mantovaara, T.; Pertoft, H.; Porath, J. *Biotechnology and Applied Biochemistry* **1989**, *11*, 564-570.
34. Chaouk, H.; Hearn, M.T.W. *Journal of Biochemical and Biophysical Methods* **1999**, *39*, 161-177.
35. Holmes, L.D.; Schiller, M.R. *Joyrnal of Liquid Chromatography and Related Techniques* **1997**, *20*, 123-142.
36. Andersson, L. *International Journal of Bio-Chromatography* **1996**, *2*, 25-36.
37. Zachariou, M.; Hearn, M.T.W. *Biochemistry* **1996**, *35*, 202-211.
38. Sulkowski, E. *Makromolekular Chemistry, Macromolecular Symposium* **1988**, *17*, 335-348.
39. Johnson, R.D.; Todd, R.J.; Arnold, F.H. *Journal of Chromatography A* **1996**, *725*, 225-235.
40. Li, Y.; Agrawal, A.; Sakon, J.; Beitle, R. *Journal of Chromatography A* **2001**, *909*, 183-190.

References

41. Porath, J. *International Journal of Bio-Chromatography* **2001**, 6, 51-78.
42. Chen, W.-Y.; Wu, C.-F.; Liu, C.-C. *Journal of Colloid and Interface Science* **1996**, 180, 135-143.
43. Belew, M.; Porath, J. *Journal of Chromatography* **1990**, 516, 333-354.
44. C[plankv]jaga, G.; Bochkariov, D.E.; Jokhadze, G.G.; Hopp, J.; Nelson, P. *Journal of Chromatography A* **1999**, 864, 247-256.
45. Chen, H.-M.; Luo, S.-L.; Chen, K.-T.; Lii, C.-K. *Journal of Chromatography A* **1999**, 852, 151-159.
46. Bornhorst, J.A.; Falke, J.J. *Methods in Enzymology* **2000**, 326, 245-254.
47. Ivanov, A.E.; Galaev, I.Y.; Kazakov, S.V.; Mattiasson, B. *Journal of Chromatography A* **2001**, 907, 115-130.
48. Kumar, A.; Galaev, I.Y.; Mattiasson, B. *Journal of Chromatography B* **2000**, 741, 103-113.
49. Zaveckas, M.; Baskeviciute, B.; Luksa, V.; Zvirblis, G.; Chmieliauskaite, V.; Bumelis, V.; Pesliakas, H. *Journal of Chromatography A* **2000**, 904, 145-169.
50. Sivars, U.; Abramson, J.; Iwata, S.; Tjerneld, F. *Journal of Chromatography B* **2000**, 743, 307-316.
51. Kröger, D.; Liley, M.; Schiweck, W.; Skerra, A.; Vogel, H. *Biosensors & Bioelectronics* **2001**, 14, 155-161.
52. Brandt, S.; Goffe, R.A.; Kessler, S.B.; O'Connor, J.L.; Zale, S.E. *Bio/technology* **1988**, 6, 779-782.
53. Kubota, n.; Nakagawa, Y.; Eguchi, Y. *Journal of Applied Polymer Science* **1996**, 62, 1153-1160.
54. Serafica, G.C.; Pimbley, J.; Belfort, G. *Biotechnology and Bioengineering* **1994**, 43, 21-36.
55. Hari, P.R.; Paul, W.; Sharma, C.P. *Journal of Biomedical Materials Research* **2000**, 50, 110-113.
56. Denizli, A.; Tanyolaç, D.; Salih, B.; Aydinlar, E.; Özdural, A.; Piskin, E. *Journal of Membrane Science* **1997**, 137, 1-8.
57. Arica, M.Y.; Denizli, A.; Baran, T.; Hasirci, V. *Polymer International* **1998**, 46, 345-352.
58. Arica, M.Y.; Denizli, A. *Separation Science and Technology* **2000**, 35, 2243-2257.

References

59. Grasselli, M.; Navarro del Cañizo, A.A.; Campari, S.A.; Wolman, F.J.; Smolko, E.E.; Cascone, O. *Radiation Physics and Chemistry* **1999**, *55*, 203-208.
60. Reif, O.-W.; Nier, V.; Bahr, U.; Freitag, R. *Journal of Chromatography A* **1994**, *664*, 13-25.
61. Camperi, S.A.; Grasselli, M.; Cascone, O. *Bioseparation* **2000**, *9*, 173-177.
62. Ho, C.-H.; Limberis, L.; Caldwell, K.D.; Steward, R.J. *Langmuir* **1998**, *14*, 3889-3894.
63. Takeshita, T.; Shimohara, T.-A.; Maeda, S. *Journal of the American Organic Chemistry Society* **1982**, *59*, 104-107.
64. Staab, H.A.; Walther, G.; Rohr, W. *Berichte* **1962**, *95*, 2073-2075.
65. Takeshita, T.; Wakebe, I.; Maeda, S. *Journal of the American Organic Chemistry Society* **1980**, *Dec*, 430-434.
66. Trost, B.; Flemming, I. *Comprehensive Organic Synthesis*; Vol. 6, Pergamon Press: Oxford. pp 631-701.
67. March, J. *Advanced Organic Chemistry, 4th Edition*; Wiley-Interscience: New York. pp 395-420.
68. Rautenbach, M. *P.h.D. Thesis*. 2.1-2.24. 1999. Stellenbosch University.
69. Bredenkamp, M.W.; Holzapfel, C.W.; Van Zyl, W.J. *Liebigs Annalytical Chemistry*. **1990**, 871-875.
70. Yamada, S.; Kasai, Y.; Shiori, T. *Tetrahedron Letters* **1973**, *18*, 1595-1598.
71. Lowe, C.R.; Dean, P.D.G. *Affinity Chromatography*; Wiley-Interscience: London, 2001;
72. Christian, G.D. *Analytical Chemistry*; John Wiley & Sons: New York, 1994;
73. Liebenberg, L. *M.Sc. Thesis*. 2001. Stellenbosch University.
74. Furniss, B.S.; Hannaford, A.J.; Smith, P.W.G.; Tatchell, A.R. *Vogel's Textbook of Practical Organic Chemistry, 5th Edition*; Longman Scientific and Technical: Essex, England, 1998; pp 401-409.
75. Averill, D.F.; Legg, J.I.; Smith, D.L. *Inorganic Chemistry* **1972**, *11*, 2344-2349.
76. Yanic, C.; Bredenkamp, M.W.; Jacobs, E.P.; Spies, H.S.C.; Swart, P. *Journal of Applied Polymer Science* **2000**, *78*, 109-117.
77. Forster, M.; Vahrenkamp, H. *Chemical Berichte*. **1995**, *128*, 541-550.

78. Halloran, L.J.; Caputo, R.E.; Willett, R.D.; Legg, J.I. *Inorganic Chemistry* **1975**, *14*, 1762-1767.
79. Radanovic, D.J.; Douglas, B.E. *Journal of Coordination Chemistry*. **1975**, *4*, 191-198.
80. Radanovic, D.J.; Matovic, V.C.; Matovic, Z.D.; Battaglia, L.P.; Pelizzi, G.; Ponticelli, G. *Inorganica Chimica Acta* **1995**, *237*, 151-157.
81. Radanovic, D.J.; Prelesnik, B.V.; Radanovic, D.D.; Matovic, Z.D.; Douglas, B.E. *Inorganica Chimica Acta* **1997**, *262*, 203-211.
82. Yang, L.; Wang, G.; Yan, S.; Liao, D.; Jiang, Z.; Shen, P.; Wang, H.; Wang, R.; Yao, X. *Polyhedron* **1993**, *12*, 1793-1795.
83. Orpen, A.G.; Brammer, L.; Allen, F.H.; Kennard, O.; Watson, D.G.; Taylor, R. *Journal of the Chemical Society, Dalton Transactions* **1989**, *Suppliment*, S1-S83.
84. Baron, D.; Hering, J.G. *Journal of Environmental Quality* **1998**, *27*, 844-850.